

Review

# Catalytic Properties of the Spinel-Like $\text{Cu}_x\text{Mn}_{3-x}\text{O}_4$ Copper Manganese Oxides—An Overview

László Kótai <sup>1,\*</sup>, Vladimir M. Petruševski <sup>2</sup>, Laura Bereczki <sup>1</sup> and Kende Attila Béres <sup>1,3</sup>

<sup>1</sup> Institute of Materials and Environmental Chemistry, Research Centre for Natural Sciences, Magyar Tudósok Krt. 2, H-1117 Budapest, Hungary

<sup>2</sup> Faculty of Natural Sciences and Mathematics, Ss. Cyril and Methodius University, NM-1000 Skopje, North Macedonia

<sup>3</sup> György Hevesy PhD School of Chemistry, Institute of Chemistry, ELTE Eötvös Loránd University, Pázmány Péter s. 1/A, H-1117 Budapest, Hungary

\* Correspondence: kotai.laszlo@ttk.hu

**Abstract:** Copper manganese oxide spinels and related (multiphase) materials with the formula  $\text{Cu}_x\text{Mn}_{3-x}\text{O}_4$  are the active catalysts in a wide variety of industrially important processes due to their great diversity in their phase relations, metal ion valence/site distribution, and chemical properties. In this review, we summarize the preparation methods and their effects on the composition, properties, and catalytic properties of various  $\text{Cu}_x\text{Mn}_{3-x}\text{O}_4$  catalysts with various Cu/Mn ratios. The main summarized catalytic reactions are the oxidation of carbon monoxide, nitrogen oxide, and hydrogen sulfide and the oxidative removal of organic solvents such as benzene, toluene, and xylene from the air. Some industrially important reactions (steam reforming of methanol or synthesis gas) and the manufacture of organic chemicals (methyl formate, propylene oxide, and benzyl alcohol) catalyzed by  $\text{Cu}_x\text{Mn}_{3-x}\text{O}_4$  spinels are also reviewed.

**Keywords:** copper manganite; spinel; catalyst; synthesis; carbon monoxide; steam reforming; valence distribution; aromatic hydrocarbons oxidation; synthesis gas; air purification



**Citation:** Kótai, L.; Petruševski, V.M.; Bereczki, L.; Béres, K.A. Catalytic Properties of the Spinel-Like  $\text{Cu}_x\text{Mn}_{3-x}\text{O}_4$  Copper Manganese Oxides—An Overview. *Catalysts* **2023**, *13*, 129. <https://doi.org/10.3390/catal13010129>

Academic Editors: Filippo Bossola and Nicola Scotti

Received: 13 December 2022

Revised: 31 December 2022

Accepted: 4 January 2023

Published: 6 January 2023



**Copyright:** © 2023 by the authors. Licensee MDPI, Basel, Switzerland. This article is an open access article distributed under the terms and conditions of the Creative Commons Attribution (CC BY) license (<https://creativecommons.org/licenses/by/4.0/>).

## 1. Introduction

From both fundamental and applicative points of view, copper manganese oxides, especially the copper manganese spinel compounds and related (multiphase) materials with  $\text{Cu}_x\text{Mn}_{3-x}\text{O}_4$  formula, are important catalysts because of their great diversity in their phase relations, metal ion valence/site distribution, and chemical properties. Copper and manganese oxide-based materials are widely used catalysts in many industrially important processes such as room-temperature CO conversions, exhaust gas purification, oxidation of harmful organic pollutants, and methanol conversions [1–5]. The most important representatives of the system are the  $\text{Cu}_{0.5}\text{Mn}_{2.5}\text{O}_4$ ,  $\text{CuMn}_2\text{O}_4$ , and  $\text{Cu}_{1.5}\text{Mn}_{1.5}\text{O}_4$  phases, but the solid solutions of  $\text{Cu}_x\text{Mn}_{3-x}\text{O}_4$  spinels ( $0 < x < 3$ ), and composite materials with inhomogeneous phase distribution are also known, which have special properties due to stresses in the mixed crystals/solid solutions/phase boundaries [1–5].

Hopcalite was the first copper manganese oxide catalyst used in the long term for CO removal from air [6], and depending on the production conditions, may contain various amounts and kinds of  $\text{Cu}_x\text{Mn}_{3-x}\text{O}_4$  spinels together with copper, manganese, and copper manganese oxides. The presence of  $\text{Cu}_x\text{Mn}_{3-x}\text{O}_4$  components in various copper manganese oxide-based catalysts strongly depends on the synthesis conditions, and sometimes on the catalytic reaction condition due to the reductive/oxidative nature of the atmosphere, and reactants also have a strong influence on the composition/phase relations of the catalysts used. The crystallinity, composition, and chemical state of phases and surface layers in  $\text{Cu}_x\text{Mn}_{3-x}\text{O}_4$  catalysts, including the presence of amorphous materials, distorted crystal lattices, and the number of oxygen and metal vacancies are key parameters

in the development of catalysts with high activity. The newest trends belong to the so-called “defect and synergic engineering” methods with the aim of enhancing the oxygen replenishment capacity of  $\text{Cu}_x\text{Mn}_{3-x}\text{O}_4$  phases. The amount and distribution of copper and oxygen vacancies are regulated with the preparation and annealing conditions. The valence of copper and manganese ions and the distribution of the  $\text{Cu}^{\text{I,II}}$  and  $\text{Mn}^{\text{II,III,IV}}$  ions between the crystalline and amorphous phases are key parameters, both in the bulk and surface layer, including the distribution of these ions between the tetrahedral and octahedral spinel sites. These features of  $\text{Cu}_x\text{Mn}_{3-x}\text{O}_4$  spinels can be controlled with a wide variety of reaction and annealing conditions, including the reaction routes, Cu/Mn ratios, metal valences, counter-ions, reagents, metal compound concentrations, temperature, time, and other factors.

In this review, we focused on the effect of synthesis routes (and consequently, the composition and structure) on the catalytic efficiency of  $\text{Cu}_x\text{Mn}_{3-x}\text{O}_4$  spinels. We summarized the influence of the preparation conditions on the composition, structure, and catalytic properties of  $\text{Cu}_x\text{Mn}_{3-x}\text{O}_4$  spinels and mixed-phase composites with various Cu/Mn ratios containing  $\text{Cu}_x\text{Mn}_{3-x}\text{O}_4$  spinel components (Tables 1–3). It is a widely accepted fact that the  $\text{Cu}_x\text{Mn}_{3-x}\text{O}_4$  spinel phase is one of the main active phases in the mixed Mn–Cu oxides in various catalytic oxidation reactions [7,8]. The adsorbed surface oxygen concentration and the  $\text{Cu}^{2+} + \text{Mn}^{3+} \leftrightarrow \text{Cu}^+ + \text{Mn}^{4+}$  redox cycle play a key role in these processes, and oxygen vacancies that form ensure the regeneration ability of the copper manganese oxide catalysts. The presence and activity of the active spinel phases depend on the distribution of ions between the crystalline sites, indirectly on the synthesis conditions. Therefore, we summarized and compared the influence of the synthetic routes (ceramic, precipitation, redox, and combined methods) on the composition and catalytic properties of the copper manganese oxide spinel catalysts.

The reviewed catalytic reactions were the oxidation of carbon monoxide (Table 4), the removal of organic and inorganic volatiles such as benzene, toluene, trichloroethylene, NO, or  $\text{H}_2\text{S}$  from air (Tables 5–9), the manufacturing of some organic chemicals (methyl formate, propylene oxide, and benzyl alcohol) (Tables 10–12) and the steam reforming of methanol (hydrogen production) (Table 13). These examples show the enormous industrial and environmental protection significance of these cheap and easily available noble metal-free spinel catalysts that contain copper and manganese oxide. Defect and synergism engineering can develop new kinds of copper manganese oxide catalysts with increased efficiency and selectivity in various reactions. Doping the known and newly prepared copper manganese oxide spinels is a prospective field of modifying and developing new noble metal-free catalyst systems.

## 2. Preparation Routes of $\text{Cu}_x\text{Mn}_{3-x}\text{O}_4$ Spinels

The main spinel preparation methods consist of solid-phase reactions of copper and manganese oxides. These oxides can be prepared in situ from their precursors (hydroxide, carbonate, oxalate, or other compounds) precipitated from solutions with precipitation, gel-forming, and redox precipitation [9–13]. A special case of the stoichiometric  $\text{CuMn}_2\text{O}_4$  synthesis is based on a solid-phase thermal decomposition of copper permanganate or its complexes with reducing ligands like ammonia [14].

The calculated Cu–Mn–O<sub>2</sub> phase diagram shows the temperature–composition relationships [10] (Figure 1).

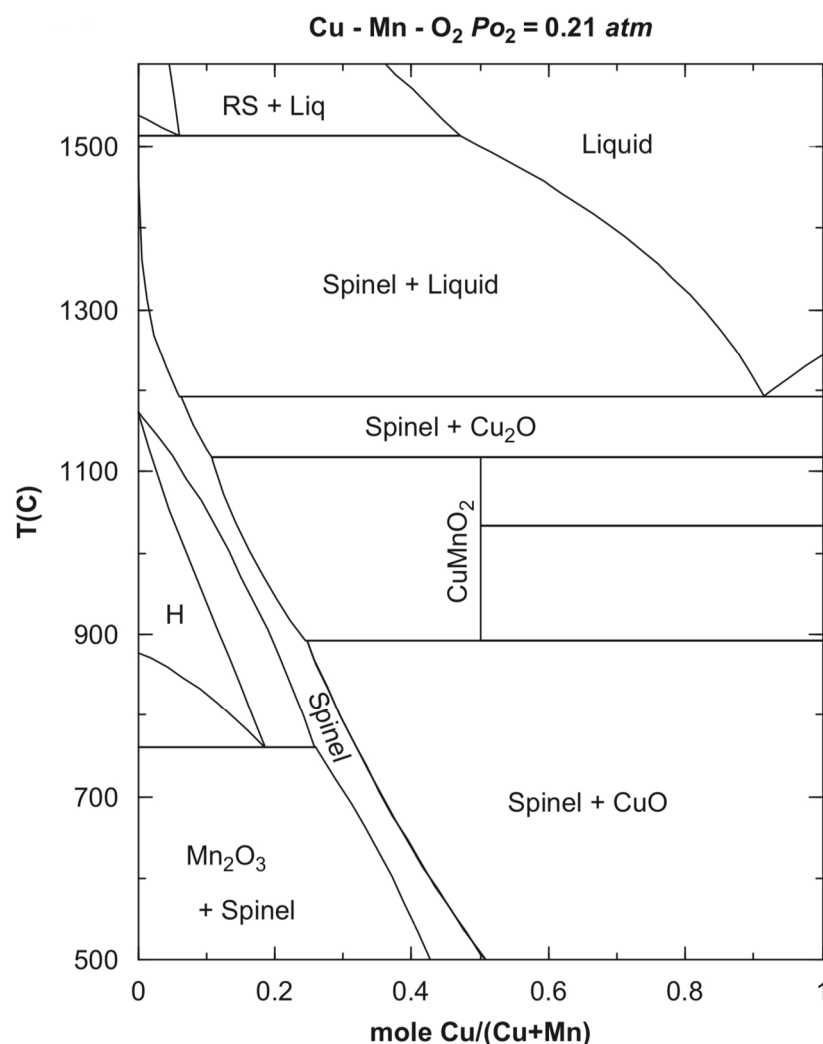


**Figure 1.** The calculated phase diagram of the Cu–Mn–O<sub>2</sub> system (reproduced from [10]).

In order to ensure homogeneous distribution of the reacting precursors, various methods have been developed over the simple grinding of oxide precursors, e.g.,

- precipitation of copper and manganese hydroxides or carbonates or oxalates directly from aqueous solutions with bases or with special techniques such as spray drying, immersion, or alginate xerogel formation
- hydrothermal and solvothermal methods with the transformation of the precursors containing metal into reactive materials; these methods include hydrolysis or co-precipitation with alkaline materials, such as ammonia that formed from the hydrolysis of urea or hexamethylenetetramine
- solution and solid–phase redox reactions, such as oxidation of low-valence Cu or Mn compounds with permanganate or other oxidants, with subsequent heat treatment or the thermal decomposition of copper permanganate or its complexes that have reducing ligands such as ammonia.

### 2.1. Ceramic and Related Processes from Solid Precursors

The stability area of the Cu<sub>x</sub>Mn<sub>3–x</sub>O<sub>4</sub> spinels (Figure 2) shows that compounds with  $x > 1$  at atmospheric oxygen pressure can be prepared from the corresponding copper and manganese oxides only above 900 °C. The copper-rich spinels such as Cu<sub>1.5</sub>Mn<sub>1.5</sub>O<sub>4</sub> ( $x = 1.5$ ) can be prepared below 900 °C only at elevated oxygen pressures, but due to the rather slow diffusion of copper and manganese ions in oxides below 900 °C, long enough sintering time

and/or highly reactive precursors have to be used. In the preparation of manganese-rich spinels, such as  $\text{CuMn}_2\text{O}_4$  ( $x = 1$ ), the clustering of  $\text{Mn}^{\text{III}}$  ions causes complications [9].

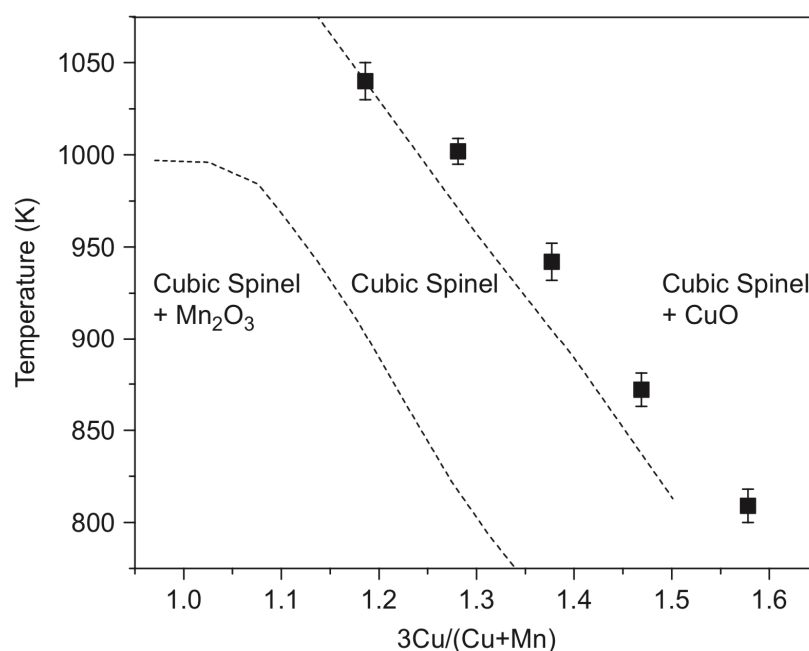


**Figure 2.** Stability region of the cubic spinels in the Cu–Mn–O system in air (reproduced from [9]).

The high-temperature sintering of the finely divided copper and manganese oxides in the appropriate ratio is the most suitable method for the preparation of compounds  $\text{Cu}_x\text{Mn}_{3-x}\text{O}_4$  with  $x \sim 1.0$ , because the reaction temperature can be selected as high as possible (Figure 2) [9]. For example,  $\text{Cu}_x\text{Mn}_{3-x}\text{O}_4$  compounds with  $0.98 < x < 1.10$  were prepared by sintering the mixtures of  $\text{CuO}$  and  $\text{Mn}_3\text{O}_4$  in air at temperatures between 900 and 940 °C for 72 h. Quenching in water resulted in samples of slightly tetragonally distorted spinels with  $x < 1.06$ , whereas at  $x > 1.06$  values (higher copper concentrations), cubic spinels are produced [9]. Spray granulation of  $\text{CuO}$  and  $\text{Mn}_3\text{O}_4$  in a spouted bed system in a molar ratio of 1:2 with subsequent calcination at 1125 °C for 2 h resulted in  $\text{Cu}_{1.5}\text{Mn}_{1.5}\text{O}_4$  [15]. A solid-state reaction of  $\text{CuO}$  and  $\text{MnO}_2$  powders mixed in the desired proportions resulted in  $\text{Cu}_x\text{Mn}_{3-x}\text{O}_4$  spinels with  $x = 1.1$ – $1.6$  at 940 °C for 24 h in air with intermittent grindings [10]. Two cubic spinels,  $\text{Cu}_{1.15}\text{Mn}_{1.85}\text{O}_4$  and  $\text{Cu}_{1.47}\text{Mn}_{1.53}\text{O}_4$ , were prepared similarly in the presence of 5 wt.% graphite as a pore-modifier additive at 950 °C for 6 h. These spinels contained macropores formed by the evolved  $\text{CO}_2$  gas [12]. Precursors of metal oxides, e.g., copper and manganese carbonates mixed at Mn:Cu 3:1, 1:1, and 1:3 ratios, were used to prepare Cu–Mn spinels by heating at 750 and 1000 °C [11,16]. The stoichiometric  $\text{CuMn}_2\text{O}_4$  was prepared analogously at 700 °C for 240 h [17]. Spray-drying of water-soluble precursors, e.g., metal nitrates, ensured avoiding macroscopic separation. The homogeneous aq. solution of copper(II) and manganese(II) nitrate mixtures were nebulized and dried with a hydrogen burner at 300 °C. The obtained solid mixed metal nitrate particles were partially decomposed into oxides when kept at 350 °C for 24 h. A series of cubic  $\text{Cu}_x\text{Mn}_{3-x}\text{O}_4$  spinels with  $1.1 < x < 1.5$  [9] was prepared in this way.

A supported mixed-phase  $\text{Cu}_{1.4}\text{Mn}_{1.6}\text{O}_4$  catalyst with  $\text{CuO}$  and/or  $\text{Mn}_2\text{O}_3$  content was synthesized by incipient wetness impregnation with the use of copper nitrate trihydrate and manganese(I) nitrate tetrahydrate and anatase. The aqueous solutions were mixed with anatase, the mixture was dried at 100 °C for 5 h, and calcined at 500 °C for 7 h in air [18].

A mechanochemical route to prepare solid spinel precursors was also developed [19]. Solid  $\text{Mn}(\text{CH}_3\text{COO})_2 \cdot 4\text{H}_2\text{O}$ , copper acetate  $\text{Cu}(\text{CH}_3\text{COO})_2 \cdot 4\text{H}_2\text{O}$ , and oxalic acid ( $\text{H}_2\text{C}_2\text{O}_4 \cdot 2\text{H}_2\text{O}$ ) were ball-milled in a molar ratio of  $\text{Mn}^{\text{II}}:\text{Cu}^{\text{II}}:\text{oxalic acid}$  of  $1 - x:x:0.5$

( $x = 0, 0.1, 0.2, 0.3, 0.4,$  and  $0.5$ ) at room temperature for 3 h. The powdered mixture was calcined at  $550\text{ }^{\circ}\text{C}$  for 2 h in air [19]. A similar process based on oxalate precursor formation is when solid  $\text{Cu}_2\text{CO}_3(\text{OH})_2$  and  $\text{MnCO}_3$  were premixed in a 1:2 molar ratio with 20% stoichiometric excess of solid oxalic or citric acid, and the mixtures were ground under ambient conditions in a planetary mill at a speed of 600 rpm for 2 h. Calcination at 300 and  $500\text{ }^{\circ}\text{C}$  in air for 4 h resulted in  $\text{CuMn}_2\text{O}_4$  [20].

A short summary of the ceramic (solid-state) preparation methods of catalysts containing  $\text{Cu}_x\text{Mn}_{3-x}\text{O}_4$  phases is given in Table 1. The solid-phase thermal decomposition of copper permanganates is discussed separately.

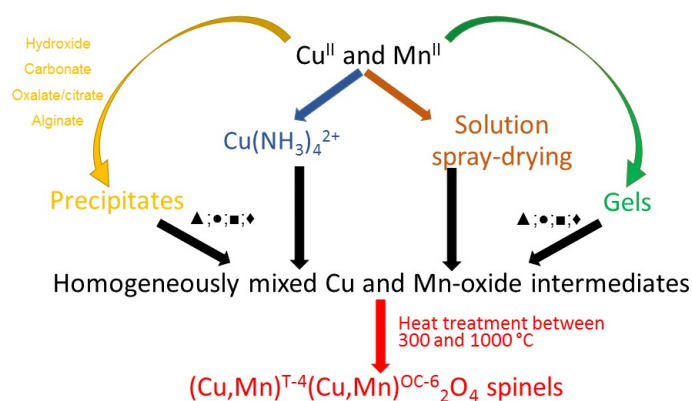
**Table 1.** Synthesis conditions of  $\text{Cu}_x\text{Mn}_{3-x}\text{O}_4$  catalysts with solid-phase methods.

$x$	Precursors	Synthesis/Annealing Conditions	[Ref.]
0.98–1.10	$\text{CuO}, \text{Mn}_3\text{O}_4$	In air, $800\text{--}940\text{ }^{\circ}\text{C}$ , 72 h, quenching in $\text{H}_2\text{O}$	[9]
1.5	$\text{CuO}, \text{Mn}_3\text{O}_4$	Spray granulation, calcining at $1125\text{ }^{\circ}\text{C}$ for 2 h	[15]
1.1–1.6	$\text{CuO}, \text{MnO}_2$	Grinding, pressing, $940\text{ }^{\circ}\text{C}$ for 24 h, annealing between $500$ and $850\text{ }^{\circ}\text{C}$	[10]
1.15–1.47	$\text{CuO}, \text{MnO}_2$	5 wt.% graphite as pore modifier, $950\text{ }^{\circ}\text{C}$ for 6 h	[12]
0.98–1.10	$\text{CuO}, \text{MnCO}_3 \cdot \text{H}_2\text{O}$	In air, $800\text{--}940\text{ }^{\circ}\text{C}$ , 72 h, quenching in $\text{H}_2\text{O}$	[21]
1	$\text{CuCO}_3 \cdot \text{Cu}(\text{OH})_2, \text{MnCO}_3$	Heating at $750$ and $1000\text{ }^{\circ}\text{C}$	[16]
1.5	$\text{CuCO}_3 \cdot \text{Cu}(\text{OH})_2, \text{MnCO}_3$	20% excess of solid oxalic or citric acid, grinding at 600 rpm for 2 h, calcining at $300\text{--}500\text{ }^{\circ}\text{C}$ in air for 4 h	[20]
1	$\text{Cu}(\text{II})$ and $\text{Mn}(\text{II})$ nitrates	Heating in air to decompose into oxides then calcining at $700\text{ }^{\circ}\text{C}$ for 240 h	[17]
1	$\text{Cu}(\text{II})$ acetate tetrahydrate, $\text{Mn}(\text{II})$ acetate tetrahydrate	Oxalic acid dihydrate, ball milling at room temperature for 3 h, calcining at $550\text{ }^{\circ}\text{C}$ for 2 h in air	[19]

The solid-state methods started from oxides or carbonate, or nitrate oxide precursors require elevated temperatures ( $>700\text{ }^{\circ}\text{C}$ ); thus these methods are favorable for preparing crystalline spinels (Table 1). The spinels with  $x = 0.98\text{--}1.6$  can be prepared with these solid-phase methods, and the solid precursor oxides can be homogenized with classical intermittent grindings [10] or spray drying [15]. Either cubic or tetragonally distorted spinels can be prepared by selecting the appropriate precursor composition and annealing temperature (Figures 1 and 2) [20]. Pore-forming agents such as graphite resulted in porous materials [12]. The intensive milling of the solid oxalic or citric acid with solid carbonate or acetate salts resulted in mechanochemical reactions and the formation of oxalate/citrate precursors. These precursors were transformed into  $\text{CuMn}_2\text{O}_4$  at lower temperatures ( $300\text{--}550\text{ }^{\circ}\text{C}$ ) [17,19] than the appropriate metal oxides or a mixture of oxides and carbonates ( $800\text{--}940\text{ }^{\circ}\text{C}$ ) [21], or carbonates ( $750\text{--}1000\text{ }^{\circ}\text{C}$ ) [16].

## 2.2. In Situ Precipitation of Solid Precursors from Solutions

Mixing the dissolved water-soluble precursors in solutions and their transformation in situ into homogeneously mixed solid precursors—mainly hydroxides, carbonates, or oxalates—is one of the most frequently used methods (Scheme 1). Sodium hydroxide and ammonium hydroxide or sodium and ammonium carbonates are the most frequently used precipitation agents. Water-soluble copper and manganese salts (most frequently nitrates, sulfates, chlorides, and acetates) are used as precursors containing metal [21–24].



**Special conditions:** ▲ Xerogel ● Hydrothermal ■ Solvothermal ◆ Emulsion

**Scheme 1.** Summarizing the reaction routes to prepare  $\text{Cu}_x\text{Mn}_{3-x}\text{O}_4$  spinels with methods based on precipitation.

The single-phase cubic  $\text{Cu}_x\text{Mn}_{3-x}\text{O}_4$  spinels with  $1.1 < x < 1.5$  values were prepared by sintering the co-precipitated copper and manganese hydroxide mixtures in an oxygen atmosphere between 500 and 800 °C for 48 h [9]. Similarly, the aqueous solutions containing copper and manganese acetates or nitrates (1:2 molar ratio of copper to manganese) were mixed with 4 M aq. NaOH at 298 K until the final pH of 11 was reached.  $\text{CuMn}_2\text{O}_4$  formed after 30 min aging at 298 K, drying in air at 50 °C for 24 h, and calcination at 300 °C for 2 h [25]. Instead of NaOH, organic bases can also be used, such as tetramethylammonium hydroxide.  $\text{CuMn}_2\text{O}_4$  was prepared from the aqueous solutions of  $\text{Cu}(\text{NO}_3)_2 \cdot 3\text{H}_2\text{O}$  and 2 equiv. of  $\text{Mn}(\text{NO}_3)_2 \cdot 4\text{H}_2\text{O}$  [26,27], by adding aq. tetramethylammonium hydroxide at 25 °C for 20 min, followed by drying and calcining the precipitate at 100 °C for 24 h and 400 °C for 5 h, respectively [26].

If ammonium hydroxide acts as a hydroxide ion source in the synthesis of the spinel containing Cu, the ammonia has a double role: a precipitating and a complex-forming agent. The starting salts that contain copper immediately turn into [tetraamminecopper(II)] complexes, and the precipitation of copper(II) and manganese hydroxides arises from the self-protonation of the [tetraamminecopper(II)] ion [27,28]. A series of Cu–Mn mixed oxide catalysts with Cu/Mn molar ratios of 2:1, 1.5:1, 1:1, and 0.5:1 containing  $\text{Cu}_{1.5}\text{Mn}_{1.5}\text{O}_4$  as the active phase was prepared with this method. A 1 M  $\text{Mn}(\text{NO}_3)_2$  aqueous solution with pH = 3–4 was dropped into an ammoniacal copper salt solution with pH = 9–10 at 30–40 °C. The precipitate was aged for 5 h and then calcined at 550 °C for 4 h [29,30]. The ammonia can also be generated in situ in hydrothermal/solvothermal reactions of urea or hexamethylenetetramine [13,31]. The advantages of the precipitation methods are combined with the positive effect of harsh reaction conditions (high temperature and pressure), and the hydrolysis with  $\text{H}_2\text{O}$ . A hydrothermal reaction was used to prepare mixed oxide phases containing  $\text{Cu}_{1.5}\text{Mn}_{1.5}\text{O}_4$  with an overall Cu/Mn ratio < 0.2 from copper nitrate, manganese nitrate, citric acid, urea, and a  $\text{KMnO}_4$  solution ( $\text{Mn}(\text{NO}_3)_2/\text{KMnO}_4$  and urea/citric acid/ $\text{Mn}^{\text{II}}$  +  $\text{KMnO}_4/\text{Cu}$  ratios were 1:2 and 1.5:1.5:1:0–0.2, respectively). Aqueous ammonia solution was added dropwise until a pH of 6–7 was reached. Then, the mixture was heated at 180 °C for 12 h in an autoclave. The precipitate was dried and calcined at 350 °C in air for 4 h [32].

The most frequently used method to prepare Cu and Mn-containing intermediates for spinel synthesis is the precipitation of a mixture of Cu and Mn carbonates/basic carbonates with the use of water-soluble carbonate compounds, mainly with sodium and ammonium carbonate. For example,  $\text{CuMn}_2\text{O}_4$  was prepared from an aqueous solution containing copper nitrate trihydrate and manganese nitrate hexahydrate in a 1:2 molar ratio by treatment with 2 M  $\text{Na}_2\text{CO}_3$  until pH = 8.3 was reached, with subsequent calcination of the precipitate formed at 400–500 °C for 2–18 h [33]. The  $\text{Cu}_{1.5}\text{Mn}_{1.5}\text{O}_4$  spinel was prepared from copper and manganese acetates dissolved in a ratio of 1:1 in water by co-precipitation

with an aqueous solution of sodium carbonate at room temperature. The solid obtained was dried and calcined at 500 °C for 6 h. In a similar route but varying the molar ratio of Cu to Mn from 5:1 to 1:5 and the calcination temperature between 400 and 800 °C, mixed-phase catalysts with  $\text{Cu}_{1.5}\text{Mn}_{1.5}\text{O}_4$  content were prepared [34]. The effect of aging of the precipitates formed from aqueous  $\text{Cu}(\text{NO}_3)_2 \cdot 3\text{H}_2\text{O}$  and  $\text{Mn}(\text{NO}_3)_2 \cdot 6\text{H}_2\text{O}$  solutions (0.25 M each, mixed in a 1:2 ratio) at 80 °C with aqueous  $\text{Na}_2\text{CO}_3$  (0.25 M) at pH = 8.9 was studied in detail.  $\text{Cu}_{1.4}\text{Mn}_{1.6}\text{O}_4$  and  $\text{CuMn}_2\text{O}_4$  spinels were formed (80 °C, pH = 8.9) by aging the precursor precipitate between 0 to 1440 min, after drying (120 °C, 16 h) and calcination at 500 °C for 17 h. [35]. Different variations in the  $\text{Na}_2\text{CO}_3$  and metal salts concentrations, heat treatment times, and temperatures were used to prepare Cu–Mn spinels with various properties from nitrate salts of manganese and copper (80 °C, pH = 8.3, calcination at 700 °C for 7 h [36] and pH = 8.5, drying in air at 110 °C for 12 h, calcination at 300 or 500 °C in air for 4 h [20]) with an aqueous solution of  $\text{Na}_2\text{CO}_3$  as precipitation agent. Instead of sodium carbonate, ammonium carbonate can also be used, especially in preparing metal-doped spinels to avoid odium contamination. For example, La-doped  $\text{Cu}_{1.5}\text{Mn}_{1.5}\text{O}_4$  was also prepared by co-precipitation from  $\text{Mn}(\text{CH}_3\text{COO})_2 \cdot 4\text{H}_2\text{O}$  and  $\text{Cu}(\text{NO}_3)_2 \cdot 3\text{H}_2\text{O}$  solutions spiked with  $\text{La}(\text{NO}_3)_3 \cdot 6\text{H}_2\text{O}$  in a water bath at 60 °C with 1.5 M  $(\text{NH}_4)_2\text{CO}_3$  solution at a pH of 8. Calcination was done at 550 °C in air for 2 h [37].

Polycarboxylic acids such as citric acid or oxalic acid (or its precursor, e.g., ethylene glycol, under oxidative conditions) are used as precipitating and complex or gel-forming reagents in Cu–Mn spinel synthesis. The mixed copper–manganese oxalates, as thermally easily decomposable and reactive compounds, are important precursors of direct spinel synthesis. According to this, copper and manganese nitrates were dissolved in water and mixed with an aq. solution of oxalic acid in 20% excess at room temperature. The precipitate was dried at 110 °C overnight and calcined at 300–500 °C for 4 h [20]. Gel/xerogel/polymer forming is also a convenient way to prepare homogeneously mixed quasi–solid precursors with a controlled Cu and Mn salt content.  $\text{Cu}_{1.5}\text{Mn}_{1.5}\text{O}_4$  and its composites with CuO (50 and 77% CuO) were prepared with the use of 2% ionotropic sodium alginate and 0.1 M (total metal salt)  $\text{CuCl}_2$  and  $\text{MnCl}_2$  solutions in various (including 1:1) Cu:Mn stoichiometric ratios by stirring at room temperature for 12 h and by subsequent alcoholic dehydration (with increasing alcohol concentration from 10 to 100%). The xerogel formed was calcined at 450 °C for 8 h [38]. A gel-like intermediate was prepared from citric acid monohydrate, copper nitrate trihydrate, and a 50% aq. manganese(II) nitrate solution (the nitrate: citric acid molar ratio was 1:1.2) and ethylene glycol (the nitrate:ethylene glycol molar ratio was 1:3). The mixture was stirred at 70 °C, and the gel that formed was calcined at 500 °C for 3 h [19]. Copper and manganese nitrates were dissolved in a mixture of ethylene glycol, water, and concentrated nitric acid. The solution was stirred under reflux (105 °C) for 2 h and dried at the same temperature for 16 h [39]. The method resulted in the formation of polymeric precursors consisting of ethylene glycol and its oxidation product (oxalic acid). The drying procedure was adjusted to the different hydrolysis rates of the precursor complexes resulting in variations in phase compositions and crystallinity. Calcination was done at a temperature of 350 and 500 °C for 5 h [39].

A simple way to prepare  $\text{Cu}_x\text{Mn}_{3-x}\text{O}_4$  spinels is based on the autoignition of a mixed solution of urea with manganese nitrate and copper nitrate (75% excess of urea) in an open muffle furnace at 550 °C for 1 h [36,40]. Manganese(II) acetate and a calculated amount of copper nitrate (and dopant metal precursors) were dissolved in water, then a  $\text{KMnO}_4$  solution was added at room temperature, then the precipitate that formed was calcined to  $\text{Cu}_x\text{Mn}_{3-x}\text{O}_4$  spinels in air at 300 °C for 2 h [41]. The precipitation agent (ammonia) can be prepared in situ from the hydrolysis of hexamethylenetetramine [13].

The results of the preparation of  $\text{Cu}_x\text{Mn}_{3-x}\text{O}_4$  spinels from precursors made in solution-phase reactions are summarized in Table 2.

**Table 2.** Synthesis conditions of  $\text{Cu}_x\text{Mn}_{3-x}\text{O}_4$  catalyst with solution-phase methods.

$x$	Precursors	Synthesis/Annealing Conditions	[Ref.]
0.30–1.05	Cu(II) and Mn(II) nitrates	Aq. soln., 25–100% excess of urea, jellifying at 100 °C, combustion at 4–500 °C, calcining at 550 °C for 1 h	[40]
1	Cu(II) and Mn(II) nitrates	80 °C, adding of $\text{Na}_2\text{CO}_3$ , (2 M), pH = 8.3, calcining in static air at 200–400 °C for 0.5–6 h	[33]
1	Cu(II) and Mn(II) nitrates	Ethylene-glycol–water–nitric acid mixture, 2 h reflux at 105 °C, calcining at 4–500 °C for 5 h	[39]
1	Cu(II) and Mn(II) nitrates	$\text{Me}_4\text{NOH}$ , 25 °C, 20 min, drying at 100 °C for 24 h and calcining at 400 °C for 5 h	[26,42]
1–2	Cu(II) and Mn(II) nitrates	1–1 M aq. metal salts, 2 M fuel (glycerol, maleic acid, citric acid, ethyl acetoacetate, or nitric acid), 1 M NaCl, jellifying at 150 °C for 12 h, calcining at 400–700 °C for 6 h	[43]
1.1–1.5	Cu(II)- and Mn(II) nitrates	Spray-drying at 300 °C, firing at 350 °C for 24 h, sintering at 530–940 °C for 48 h, quenching in water	[9]
1.2–1.4	Cu(II) and Mn(II) nitrates	80 °C, aq. $\text{Na}_2\text{CO}_3$ , pH = 8.9, 10 min, conditioning between 0 and 1440 min at 80 °C in the mother liq., calcining at 500 °C for 17 h	[35]
1.4	Cu(II) and Mn(II) nitrates	Incipient wetness impregnation, $\text{TiO}_2$ , 100 °C for 5 h then calcining at 500 °C for 7 h in air	[18]
1.5	Cu(II) and Mn(II) nitrates	NaOH, 298 K, pH = 11, 30 min, calcining at 300 °C for 2 h	[25]
1.1–1.5	Cu(II)- and Mn(II) nitrates	NaOH, firing in air at 530–940 °C for 48 h, quenching in $\text{H}_2\text{O}$	[9,21–23]
1.5	Cu(II) and Mn(II) nitrates	Abs. ethanol, dip-coating, Al foil, room temp., drying at 300 °C for 3 h, calcining at 4–500 °C for 15–90 min	[44]
1.5	Cu(II) and Mn(II) nitrates	Urea, citric acid, 0.3 M $\text{KMnO}_4$ , pH = 6–7, 4 h, hydrothermal treatment at 180 °C for 12 h, calcining at 350 °C in air for 4 h	[32]
1.5	Cu(II) and Mn(II) nitrates	Autoignition, 75% excess of urea, open furnace at 4–500 °C, calcining at 550 °C for 1 h	[36,40]
1.5	Mn(II) and Cu(II) nitrates	Aq. $\text{Na}_2\text{CO}_3$ , 80 °C, pH = 8.3, aging at 80 °C for 6 h, calcining at 700 °C for 7 h	[36,45]
1.5	Cu(II) and Mn(II) nitrates	1.2 M $\text{Na}_2\text{CO}_3$ , 80 °C, pH = 8.5, calcining at 300–500 °C in air for 4 h	[20]
1.5	Cu(II) and Mn(II) nitrates	20% excess of aq. oxalic acid, room temperature, calcining at 300–500 °C for 4 h	[20]
0.5–2	Cu(II) and Mn(II) nitrates	Aq. citric acid, ethylene glycol, 30 °C for 2 h, jellifying at 70 °C, calcining at 500 °C for 3 h	[46]
1.5	Mn(II) nitrate, $[\text{Cu}(\text{NH}_3)_4](\text{II})$ -hydroxide	Mn nitrate (pH = 3–4) and $[\text{Cu}(\text{NH}_3)_4](\text{II})$ -hydroxide (pH = 9–10) solutions were mixed, 30–40 °C, calcining at 550 °C for 4 h	[29,30]
1.8	Mn(II) nitrate, Cu(II) acetate	Reverse microemulsion, water/triton-X100/n-octanol/cyclohexane, 25% aq. $\text{NH}_4\text{OH}$ . Stirring for 1 h, calcining at 450–1000 °C in oxygen	[47]
1.5	Mn(II) acetate, Cu(II) nitrate	Aq. $\text{Me}_4\text{NOH}$ , aging for 2 h, calcining in dry air at 400 °C for 5 h	[48]
1.5	Mn(II) acetate, Cu(II) nitrate	$\text{KMnO}_4$ , room temp., 24 h, calcining at 300 °C for 2 h	[41]
1.5	Mn(II) acetate, Cu(II) nitrate	Aq. soln., La nitrate, 1.5 M ammonium carbonate, pH = 8, 2 h aging, calcining at 550 °C for 2 h in air	[37]
1	Cu(II) and Mn(II) acetates	Aq. $\text{Na}_2\text{CO}_3$ , 80 °C, pH = 8–10, 30 min, aging at 80 °C for 12 h, calcining at 500 °C for 20 min, 10 M NaOH, hydrothermal treatment at 110 °C for 20 h, calcining at 250 °C for 1 h	[49]

**Table 2.** *Cont.*

<i>x</i>	Precursors	Synthesis/Annealing Conditions	[Ref.]
1.5	Cu(II) and Mn(II) acetates	0.2 M aq. Na <sub>2</sub> CO <sub>3</sub> , room temp., 4 h, calcining at 500 °C for 6 h	[33,34]
1.5	Cu(II) and Mn(II) acetates	NaOH, 298 K, pH = 11, 30 min, calcining at 300 °C for 2 h	[25]
1.5	Cu(II) and Mn(II) chloride	Na <sub>2</sub> CO <sub>3</sub> , 3 h aging, drying at 80 °C overnight, calcining at 450 °C for 5 h	[13]
1.5	Cu(II) and Mn(II) chlorides	Sodium alginate (2 wt.%), room temp. for 12 h, dehydration with successive ethanol–water mixture washing (10–100%), 15 min each, calcining at 450 °C for 8 h	[37]
1.2–1.5	Cu(II) and Mn(II) chlorides	pH = 4, sodium oxalate, 550–650 °C	[23,50]
1	Mn(II) sulfate, copper(II) chloride	Solvothermal method, water: methanol = 60:40, ethylene glycol, 1 M NaOH, pH = 10, 120–160 °C for 12 h	[31]
1.1–1.5	Cu(II) and Mn(II) sulfates	NaOH, firing in air at 530–940 °C for 48 h, quenching in H <sub>2</sub> O	[9,21–23]

The solution-phase spinel precursor syntheses ensure the complete distribution of copper and manganese ions and the monophasic spinel synthesis. The reactive species can be transformed into spinels at lower temperatures (>250 °C) than the solid oxides or oxide precursors. These methods are typical in the preparation of copper-rich spinels [9,13,21–23,38,50]. The copper manganese oxide spinels with  $x \geq 1$  were prepared from the appropriate sulfate, chloride, and acetate salts with such precipitating agents as NaOH, NaOH, Na<sub>2</sub>CO<sub>3</sub>, sodium oxalate, or sodium alginate. The most frequently used precursor salts are nitrate salts. For example, Cu<sub>1.5</sub>Mn<sub>1.5</sub>O<sub>4</sub> can be prepared from the Mn(II) acetate and Cu(II) nitrate via precipitating the solid precursors with ammonium carbonate or tetramethylammonium hydroxide, or with redox precipitation by KMnO<sub>4</sub> [20,37,41]. The solid precursors for the synthesis of spinels with  $x = 1.5$  and 1.8 were deposited from manganese(II) nitrate solution with the use of [tetraamminecopper(II)] hydroxide, and ammonium hydroxide (in reverse microemulsions of water–surfactant–*n*-octanol–cyclohexane) as precipitating agents, respectively [29,30,47].

The Cu<sub>*x*</sub>Mn<sub>3–*x*</sub>O<sub>4</sub> spinels with  $x = 0.3–1.5$  can be prepared from copper(II) and manganese(II) nitrate solutions with various methods. The precursors for heat treatment were precipitated with Na<sub>2</sub>CO<sub>3</sub> [20,33,35] Me<sub>4</sub>NOH [26,42], NaOH [9,21–23,25,31], or oxalic acid [20]. Direct impregnation methods including dip-coating, incipient wetness impregnation and spray drying were also used with subsequent thermal decomposition of the solid metal nitrates into active oxide precursors [9,18,44]. Gel-forming materials such as urea, an ethylene-glycol–nitric acid mixture, citric acid [32,39,46], or autoignition methods with organic fuels were also used to prepare the Cu<sub>*x*</sub>Mn<sub>3–*x*</sub>O<sub>4</sub> spinels with  $x \geq 1$  [36,40,43].

### 2.3. Thermal Decomposition of the Hydrated and Ammonia-Complexed Copper Permanganate

Anhydrous copper(II) permanganate has not been isolated yet, because the hydrated and the ammonia-complexed copper(II) permanganates decompose at lower temperatures than their ligand loss temperatures [14]. The hydrates of copper permanganate (Cu(MnO<sub>4</sub>)<sub>2</sub>·*n*H<sub>2</sub>O (*n* = 2, 3, 4, 6, 8), however, were prepared easily via various synthesis methods [14,51]. Its composition ensures an optimal Cu:Mn = 1:2 ratio to prepare the regular CuMn<sub>2</sub>O<sub>4</sub> spinel. Its thermal decomposition starts at 80 °C with oxygen evolution in an autocatalytic process [52]. The decomposition of the permanganate ion and water release are parallel processes during heating. Thus, the water content of copper permanganate (*n* = 1.7–4.1 with evaporation at 290–330 K in vacuum) does not influence the decomposition temperature or the composition of the thermal decomposition products. The product of the first decomposition step is a mixed-phase copper manganese oxide with a composition of CuMn<sub>2</sub>O<sub>5.45</sub> [53]. Kinetic studies performed in the range of 335 and 370 K showed that in the median range of thermal decomposition, the dominant decomposition feature is the

constant reaction rate without any acceleratory behavior, and the induction period was also short. The mixed-phase decomposition intermediate decomposes further when the temperature is increased to 695 K, and the amorphous product formed corresponds to the  $\text{CuMn}_2\text{O}_5$  formula. Magnetic susceptibility measurements showed that the valence state of the copper above 725 K is exclusively  $\text{Cu}^{\text{I}}$ . Thus “ $\text{CuMn}_2\text{O}_5$ ” cannot be a mixture of  $\text{CuO} + 2\text{MnO}_2$ . When the temperature was increased to 1175 K, the expected  $\text{CuMn}_2\text{O}_4$  and its partial decomposition product,  $\text{Mn}_2\text{O}_3$ , were formed [54].

The basic copper(II) permanganate,  $\text{Cu}_2(\text{OH})_3\text{MnO}_4$ , was prepared by an anion exchange of the layered  $\text{Cu}_2(\text{OH})_3\text{OAc}$  with 1 M  $\text{KMnO}_4$  in a day [55]. The thermal decomposition of  $\text{Cu}_2(\text{OH})_3\text{MnO}_4$  can be described as:

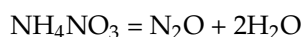


The amorphous mixed copper manganese oxide that formed catalyzes the oxidation of CO at 30 °C. The amorphous mixed copper manganese oxide crystallizes at 440 °C, and loses its catalytic activity above 500 °C but can be reactivated in oxygen at 400 °C. It decomposes at 940 °C into  $\text{CuMnO}_2$  [55].

We developed a solid-phase reaction to obtain  $\text{CuMn}_2\text{O}_4$  spinel materials with  $x = 1$  at a low temperature (between 100 and 500 °C), via a quasi-intramolecular redox reaction of the ammonia ligand and permanganate anion in  $[\text{Cu}(\text{NH}_3)_4](\text{MnO}_4)_2$  [56]. The decomposition reaction of [tetraamminecopper(II)] permanganate strongly depends on the reaction conditions. It explodes on fast heating at 65 °C and ignites at >8 atm  $\text{O}_2$  in a violent reaction (dark red flame, 1500 K combustion temperature) [57], according to the equation.



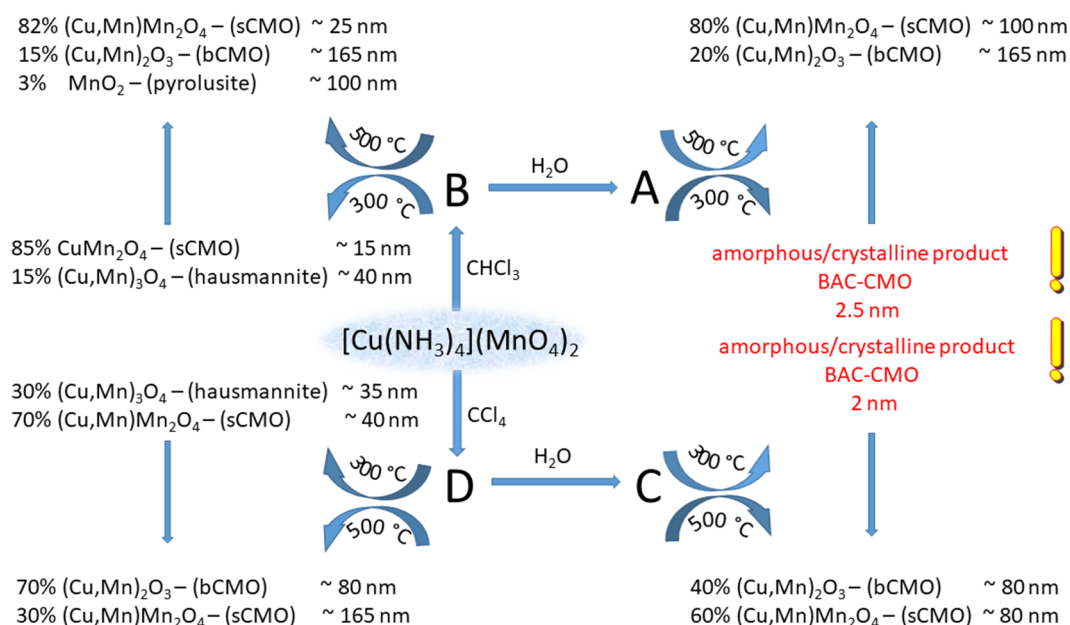
Thermogravimetric studies on the decomposition of [tetraamminecopper(II)] permanganate showed a stepwise ligand and oxygen-releasing process [58], and the solid decomposition end-product was identified on the basis of weight loss as  $\text{CuMn}_2\text{O}_4$  [58]. Although the decomposition mechanism declared was proven to be incorrect, the end-product of the decomposition was an amorphous material with  $\text{CuMn}_2\text{O}_4$  composition [56]. The decomposition residue did not dissolve in  $\text{HNO}_3$  at all, and the decomposition process was formally written as [56].



Solid-phase decomposition is frequently explosion-like; therefore, to control the decomposition process, the decomposition reaction was performed under inert solvents like  $\text{CHCl}_3$  and  $\text{CCl}_4$ . In this way, the decomposition temperature cannot exceed the boiling point of the solvent, because the evaporation heat of the solvents absorbs the exothermic reaction heat. The solid products are the expected spinel and ammonium nitrate; every other reaction product is gas. Since ammonium nitrate can be dissolved out with water and decomposed thermally as well, we studied the effect of the synthesis temperature ( $\text{CHCl}_3$ –61 °C,  $\text{CCl}_4$ –77 °C) and the isolation methods (aqueous extraction or thermal decomposition of ammonium nitrate) on the composition and properties of the resulting spinel compounds [59,60].

This temperature-limited process prevents nucleation and crystallization of the formed copper manganese oxides driven by the exothermicity-derived reaction heat (289.8 kJ/mol) [57]. The amorphous copper manganese oxides were characterized with the formula of  $\text{CuMn}_2\text{O}_{4+x}$  from  $x = 0$  ( $\text{CuMn}_2\text{O}_{4,\text{spinel}}$  structure) to  $x = 0.5$  ( $\text{Cu}_{0.89}\text{Mn}_{1.78}\square_{0.32}\text{O}_4$  or  $\text{Cu}_{0.67}\text{Mn}_{1.33}\text{MnO}_3$ ) with defect structure ( $\square$  is a defect in the spinel structure). Depending on the removal method of ammonium nitrate (washing with water or thermal decomposition) and the temperature and time of the subsequent heat treatments, the size and phase composition of the products can be controlled (Scheme 2). This method ensures a safe and

easy route to prepare copper manganese oxide nanoparticles in various compositions [60]. The samples containing copper manganese oxide and ammonium nitrate prepared in  $\text{CCl}_4$  at  $77^\circ\text{C}$  were extracted with water to remove ammonium nitrate. Subsequent heat treatment of the extraction residue up to  $400^\circ\text{C}$  for 1–8 h resulted in copper manganese oxides, which  $d(001)$  peak shows the initial stage of the formation of the spinel structure with 2 nm crystallite sizes. The crystallization of the spinels starts at  $500^\circ\text{C}$  when crystallites with the size of 80 nm were obtained [60].



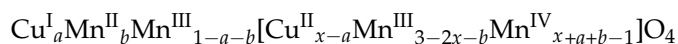
**Scheme 2.** Decomposition of [tetraamminecopper(II)] permanganate under  $\text{CHCl}_3$  (reaction products A and B) and  $\text{CCl}_4$  (reaction products C and D) with (reaction products A and C) and without (reaction products B and D) the removal of  $\text{NH}_4\text{NO}_3$  by aqueous leaching (reproduced from [60]).

### 3. Composition and Crystal Structure of $\text{Cu}_x\text{Mn}_{3-x}\text{O}_4$ Spinel

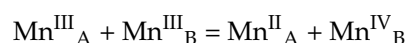
Hausmannite ( $\text{Mn}^{\text{II}}\text{Mn}^{\text{III}}_2\text{O}_4$ ) occurs in both tetragonal (room temperature) and cubic (high temperature,  $\gg 1000\text{ K}$ ) forms. The two phases co-exist in a wide temperature range [61]. The cubic spinel phase can be stabilized at lower temperatures by doping with copper [21] despite the fact that both  $\text{Mn}^{\text{III}}([\text{Ar}]d^4)$  and  $\text{Cu}^{\text{II}}([\text{Ar}]d^9)$  ions show Jahn–Teller activity in both octahedral and tetrahedral spinel sites. These  $\text{Cu}_x\text{Mn}_{3-x}\text{O}_4$  mixed oxides are solid solutions, where copper substitutes manganese in the tetragonal lattice of hausmannite ( $\text{Mn}_3\text{O}_4$ ,  $\text{Mn}^{\text{II}}\text{Mn}^{\text{III}}_2\text{O}_4$ ). Depending on the amount, site, and valence of copper ( $\text{Cu}^{\text{I}}$  or  $\text{Cu}^{\text{II}}$ ), and manganese species ( $\text{Mn}^{\text{II}}$ ,  $\text{Mn}^{\text{III}}$ , and  $\text{Mn}^{\text{IV}}$ ), distorted cubic or tetragonal spinel lattices are built up. The  $\text{Cu}_x\text{Mn}_{3-x}\text{O}_4$  spinels with  $x \approx 1$  have a tetragonally deformed structure with a  $c/a$  ratio slightly varying between 1.05 and 1.03. Above  $x = 1.06$ , a cubic spinel structure was found with a diminishing lattice parameter upon increasing copper content [9]. Formally, the stoichiometric spinel structures can be formulated as [62–64]:



In octahedral field symmetry,  $\text{Mn}^{\text{III}}$  and  $\text{Cu}^{\text{II}}$   $d$  levels are split into  $t_{2g}^3e_g^1$  and  $(t_{2g}^6)(e_g^2)e_g^1$  levels. In tetrahedral symmetry, they split into  $e^2t_2^2$  and  $(e^4)(t_2^4)(t_2^1)$ , respectively [10]. The mixing of copper and manganese valences in the spinel lattice leads to subcritical levels of Jahn–Teller active ions, thereby causing no distortion [21,65]. As a result of that, the ionic configurations in  $\text{Cu}_x\text{Mn}_{3-x}\text{O}_4$  spinels can be written as:

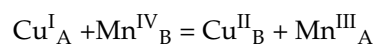


The tetrahedral sites of the spinel lattice can mainly be occupied by  $\text{Cu}^I$ ,  $\text{Mn}^{II}$ , and  $\text{Mn}^{III}$ , whereas the octahedral sites are mainly occupied by  $\text{Cu}^{II}$ ,  $\text{Mn}^{III}$ , and  $\text{Mn}^{IV}$  ions. Thus, only the  $\text{Mn}^{III}$  ions can disperse between the A (tetrahedral) and B (octahedral) spinel sites, in any proportion;  $\text{Cu}^I$  and  $\text{Mn}^{II}$  strongly favor the tetrahedral, whereas  $\text{Cu}^{II}$  and  $\text{Mn}^{IV}$  the octahedral sites. The electrical conductivity of cubic  $\text{Mn}_3\text{O}_4$  was explained by small polaron hopping between  $\text{Mn}^{III}$  and  $\text{Mn}^{III}$  on octahedral sites [66] and the disproportionation reaction between two  $\text{Mn}^{III}$  ions, resulting in  $\text{Mn}^{II}$  and  $\text{Mn}^{IV}$  [67] at the octahedral sites. The  $\text{Mn}^{II}$  in the tetrahedral sites is the consequence of the equation,



which is shifted to the  $\text{Mn}^{II} + \text{Mn}^{IV}$  side [24] in the manganese-rich compounds.

$\text{Cu}^{II}$  appeared in the octahedral site above 300 °C due to the reaction of tetrahedral  $\text{Cu}^I$  components and octahedral  $\text{Mn}^{IV}$  components [24], according to the equation.



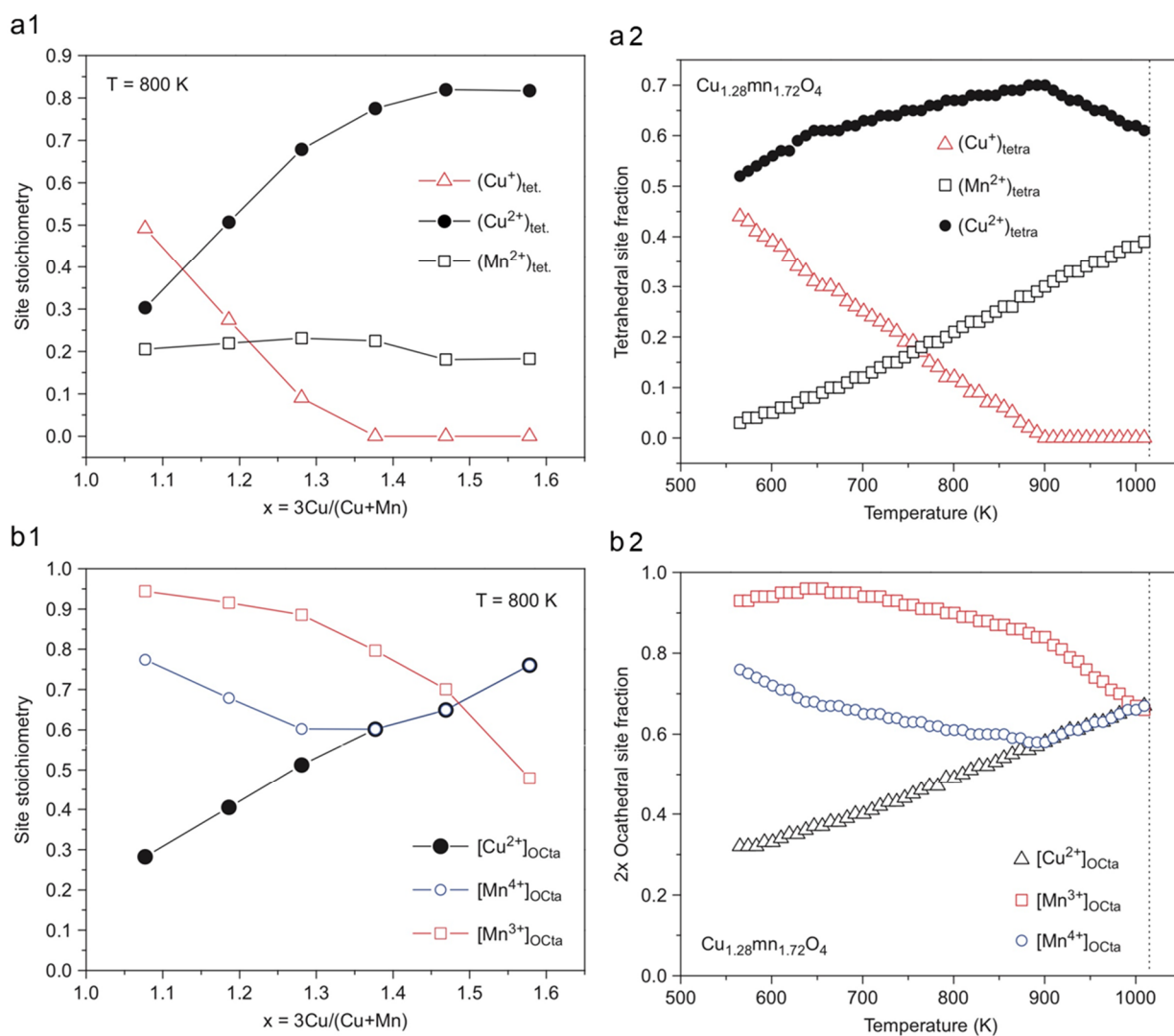
Furthermore, a thermally activated site exchange reaction was also detected by neutron diffraction measurement on the  $\text{CuMn}_2\text{O}_4$  samples quenched from 1213 K due to the strong octahedral site preference of the Jahn–Teller  $\text{Cu}^{II}$ -ion compared to that of  $\text{Mn}^{II}$  [68]. As a result of these reactions, various cation distributions were found experimentally in the samples formally from the normal ( $\text{M}^{II}\text{M}^{III}_2\text{O}_4$ ) to inverse spinel ( $\text{M}^{III}[\text{M}^{II}\text{M}^{III}]\text{O}_4$ ) structures. Therefore, the cation valence and site distributions observed at room temperature strongly depends not only on the synthesis method but also on the annealing conditions and cooling rates as well [66–72]. For example, the  $\text{CuMn}_2\text{O}_4$  crystals obtained from a 1:1 mixture of  $\text{CuO}$  and  $\text{Mn}_2\text{O}_3$  in vacuum at 1323 K and with cooling at 6 K/h to room temperature resulted in  $\text{Cu}^I_{0.2}\text{Mn}^{II}_{0.8}[\text{Cu}^{II}_{0.8}\text{Mn}^{III}_{0.2}\text{Mn}^{IV}_{1.0}]_B\text{O}_4$  [65], whereas the room temperature magnetic susceptibility measurements on quenched  $\text{CuMn}_2\text{O}_4$  showed that all Cu is monovalent, and all manganese is tetravalent [69].

Neutron diffraction experiments showed that  $\text{CuMn}_2\text{O}_4$  prepared in a solid-state reaction of oxides at 700 °C for 240 h has a partially inverted cation distribution (12–13% of copper ions located on octahedral sites [17]). Since the copper ions are mainly expected to be monovalent  $\text{Cu}^I$  at the tetrahedral sites, it means that all  $\text{Mn}^{4+}$  and  $\text{Cu}^{2+}$  ions should be located at the octahedral sites [13]. The magnetic susceptibility and Curie constant parameters of  $\text{Cu}_x\text{Mn}_{3-x}\text{O}_4$  spinels confirm the  $\text{Cu}^I(\text{T}-4)\text{Mn}^{IV}(\text{O}-6)$  configuration, and according to this, at  $x = 1.5$  ( $\text{Cu}_{1.5}\text{Mn}_{1.5}\text{O}_4$ ), the favored configuration is  $\text{Cu}^I[\text{Cu}^{II}_{0.5}\text{Mn}^{IV}_{1.0}\text{Mn}^{III}_{0.5}]_B\text{O}_4$ . The cubic structure ( $x > 1.06$ ) is an indicative parameter of the low concentration of distorting  $\text{Mn}^{III}$  and  $\text{Cu}^{II}$  cations.

The surface composition of the copper manganese oxides is not identical to their bulk composition, e.g., typically,  $\text{Cu}^{II}$  is enriched at the surface layer of  $\text{CuMn}_2\text{O}_4$  and  $\text{Cu}_{1.5}\text{Mn}_{1.5}\text{O}_4$  [44]. Thin films of copper–manganese oxides were prepared on aluminum foil by dip coating from nitrate salts dissolved in ethanol at room temperature. The coatings were decomposed and annealed at 300 °C and between 400 and 500 °C, respectively, for periods between 15 and 90 min. The results summarized in Table 3 show that the preparation method of copper manganese oxide spinels has a strong influence on the amount and distribution of the copper and manganese species with various valence at the different spinel crystal lattice sites. Furthermore, the precipitation and ceramic methods resulted in copper manganese oxide spinels with completely different metal ion valences and distributions, depending on the synthesis methods used. Not only the preparation method, but within one preparation route, the post-treatment conditions such as annealing time and temperature also have an enormous influence on the composition and properties of the  $\text{Cu}_x\text{Mn}_{3-x}\text{O}_4$  films (Figure 3).

**Table 3.** Distribution of copper ions between the T-4 and OC-6 sites of the spinel lattice in  $\text{Cu}_x\text{Mn}_{3-x}\text{O}_4$  samples.

Cu/Mn	$\text{Cu}^{\text{I}}/\text{Cu}^{\text{II}}$	$\text{Cu}^{\text{II}}$ (T-4) (A)	$\text{Cu}^{\text{II}}$ (OC-6)(B)	$\text{Cu}^{\text{I}}$ (T-4)	Preparation Method	Ref.
0.83	0.47	25	43	32	Dip-coating	[44]
0.88	0.47	25	43	32	Dip-coating	[44]
1.14	0	33	67	0	Dip-coating	[44]
1.08	0	23	77	0	Dip-coating	[44]
1.23	0.13	41	47	12	Dip-coating	[44]
2	3.16		24	76	Ceramic	[21]
2	1.00	50	25	25	Precipitation	[73]
2	2.00	0	33	66	Ceramic	[50]
2	0.39	48	24	28	Ceramic	[71]
2	0.67	0	60	40	Ceramic	[74]
1	2.00	0	33	66	Ceramic	[9,21]

**Figure 3.** Variation of the cation valence and distribution on tetrahedral and octahedral sites with temperature and composition for  $\text{Cu}_{1.28}\text{Mn}_{1.72}\text{O}_4$ . The vertical dashed line corresponds to the onset of CuO precipitation (reproduced from [10]).

For example, for the preparation of  $\text{Cu}_{1.5}\text{Mn}_{1.5}\text{O}_4$ , with the dip-coating of nitrates, the reaction has to be carried out above  $450\text{ }^\circ\text{C}$  and the full conversion of Cu and Mn oxides into  $\text{Cu}_{1.5}\text{Mn}_{1.5}\text{O}_4$  requires at least 60 min. The high conductivity of the films prepared in this way may be attributed to the presence of  $\text{Mn}^{3+}$  and  $\text{Mn}^{4+}$  in octahedral and  $\text{Cu}^+$  and  $\text{Cu}^{2+}$  in tetrahedral sites, respectively. This is detected by XPS and may be attributed to the

electron hopping between Cu<sup>I</sup> and Mn<sup>IV</sup> ions [44]. This unexpected distribution of copper valences in the film is similar to the distribution of copper valences in the surface layer of the bulk compound with the same composition.

The relative amount of copper, manganese, and the lattice defects, and also the distribution of valence states of copper and manganese ions and the locations of each type of ions at various spinel sites are one of the key factors in the catalytic activity of Cu<sub>x</sub>Mn<sub>3-x</sub>O<sub>4</sub> spinels.

#### 4. Overview of the Catalytic Activity of Cu<sub>x</sub>Mn<sub>3-x</sub>O<sub>4</sub> Spinels

One of the oldest and most important application areas of copper manganese oxide catalysts, including Cu<sub>x</sub>Mn<sub>3-x</sub>O<sub>4</sub> spinels and mixtures containing a Cu<sub>x</sub>Mn<sub>3-x</sub>O<sub>4</sub> spinel is the removal of carbon monoxide from air. The Cu<sub>x</sub>Mn<sub>3-x</sub>O<sub>4</sub> spinels, however, proved to be very active catalysts in such important processes, such as the recovery of aromatic and chlorinated hydrocarbons from air, methanol reformation to produce hydrogen, and in a series of industrially important reactions, which are summarized in Table 4, Table 5, Table 6, Table 7, Table 8, Table 9, Table 10, Table 11, Table 12 and Table 13.

**Table 4.** Removal of carbon monoxide from the air in the presence of Cu<sub>x</sub>Mn<sub>3-x</sub>O<sub>4</sub> catalysts.

Cu <sub>x</sub> Mn <sub>3-x</sub> O <sub>4</sub>	Precursors, Preparation Method, and Conditions	Catalyst Efficiency and Reaction Conditions	Refs.	Remarks
$x = 0.5$	Aq. solutions of Cu and Mn nitrates in 1/2 molar ratio were mixed, aq. NaOH solution, 298 K, pH = 11, 300 °C for 2 h	1% CO, 20% O <sub>2</sub> and 79% N <sub>2</sub> , space velocity was 20,000 mL h <sup>-1</sup> g cat <sup>-1</sup> . The temperature was ramped at a rate of 1 °C min <sup>-1</sup> from 0 °C to the final temperature, T <sub>50</sub> /T <sub>100</sub> = 80/120 °C, resp.	[25]	S <sub>BET</sub> = 46 m <sup>2</sup> g <sup>-1</sup> , V <sub>p</sub> = 0.23 cm <sup>3</sup> g <sup>-1</sup>
$x = 0.5$	Thermal decomposition of the [Cu <sub>2</sub> (OH) <sub>3</sub> MnO <sub>4</sub> ] layered basic salt	It catalyzes CO oxidation at 30 °C	[55]	Mixed phase with CuO
$x = 1.0$	Mn–nitrate, Cu–nitrate, 0.25 M each, 2 M Na <sub>2</sub> CO <sub>3</sub> , pH = 8.3, 400 for 2	5000 ppm CO in air, 25 °C, 33,000 h <sup>-1</sup> , cooling due to 10 °C adiabatic temperature increase	[33]	S <sub>BET</sub> = 93 m <sup>2</sup> g <sup>-1</sup> , mixed phase
$x = 1.0$	Metal nitrates (Cu:Mn = 1:4) in ethylene glycol–water–cc. nitric acid mixture, 2 h reflux, drying at 105 °C for 16 h, 450–500 °C	1 vol.% CO in synthetic air, 100–200 mm particles, 25 °C, flow rate: 30 000 mL h <sup>-1</sup> g <sup>-1</sup> ; Experiments with moist air were carried out near low-temperature fuel cell conditions using a different feed gas composition (1 vol.% CO, 4.88 vol.% synthetic air, 20 vol.% CO <sub>2</sub> in hydrogen), 60–120 °C, 17–20% CO conversion after 1 h	[39]	S <sub>BET</sub> = 55–67 m <sup>2</sup> g <sup>-1</sup>
$x = 1.0$	Cu–nitrate and Mn–nitrate in 1:2 ratio, 80 °C, 0.25 M Na <sub>2</sub> CO <sub>3</sub> , pH = 8.9, aging from 0 to 720 min	5% CO in He and O <sub>2</sub> (1:10 v/v) were fed to the reactor, 20 °C; total GHSV of 33,000 h <sup>-1</sup>	[35]	S <sub>BET</sub> = 26 m <sup>2</sup> g <sup>-1</sup>
$x = 1.0$	[Cu(NH <sub>3</sub> ) <sub>4</sub> ](MnO <sub>4</sub> ) <sub>2</sub> decomposition in CHCl <sub>3</sub> at 61 °C, aq. extraction, 300 °C for 1 h	0.5% CO and 0.5% O <sub>2</sub> in He, (1.37 g <sub>CO</sub> g <sub>cat</sub> <sup>-1</sup> h <sup>-1</sup> ), T <sub>10</sub> /T <sub>25</sub> /T <sub>50</sub> = 94/132/163 °C, resp.	[60]	Mixed phase
$x = 1.0$	[Cu(NH <sub>3</sub> ) <sub>4</sub> ](MnO <sub>4</sub> ) <sub>2</sub> decomposition in CHCl <sub>3</sub> at 61 °C, 300 °C for 1 h °C	0.5% CO and 0.5% O <sub>2</sub> in He, (1.37 g <sub>CO</sub> g <sub>cat</sub> <sup>-1</sup> h <sup>-1</sup> ), T <sub>10</sub> /T <sub>25</sub> /T <sub>50</sub> = 134/159/188 °C, resp.	[60]	–
$x = 1.0$	[Cu(NH <sub>3</sub> ) <sub>4</sub> ](MnO <sub>4</sub> ) <sub>2</sub> decomposition in CCl <sub>4</sub> at 77 °C, with aq. extraction (NH <sub>4</sub> NO <sub>3</sub> removal), 200–500 °C for 1–8 h	0.5% CO and 0.5% O <sub>2</sub> in He, (1.37 g <sub>CO</sub> g <sub>cat</sub> <sup>-1</sup> h <sup>-1</sup> ), without heat treatment T <sub>10</sub> /T <sub>25</sub> /T <sub>50</sub> = 121/130/161 °C, resp.; 200 °C for 1 and 8 h, T <sub>10</sub> /T <sub>25</sub> /T <sub>50</sub> = 135/155/173 °C and 127/155/177 °C, resp.; 500 °C for 1 and 8 h, T <sub>10</sub> /T <sub>25</sub> /T <sub>50</sub> = 111/142/170 and 137/164/190 °C, resp.	[60]	–
$x = 1.0$	[Cu(NH <sub>3</sub> ) <sub>4</sub> ](MnO <sub>4</sub> ) <sub>2</sub> decomposition in CCl <sub>4</sub> at 77 °C, 500 °C for 1 h	0.5% CO and 0.5% O <sub>2</sub> in He, (1.37 g <sub>CO</sub> g <sub>cat</sub> <sup>-1</sup> h <sup>-1</sup> ), T <sub>10</sub> /T <sub>25</sub> /T <sub>50</sub> = 166/190/>200 °C, resp.	[60]	–

Table 4. Cont.

$\text{Cu}_x\text{Mn}_{3-x}\text{O}_4$	Precursors, Preparation Method, and Conditions	Catalyst Efficiency and Reaction Conditions	Refs.	Remarks
$x = 1.4$	Cu–nitrate and Mn–nitrate, 1:2 ratio, 80 °C, 0.25 M $\text{Na}_2\text{CO}_3$ , pH = 8.9, aging from 0 to 300 and 1440 min	5% CO in He and $\text{O}_2$ (1:10 v/v) were fed to the reactor, 20 °C; total gas hourly space velocity of 33,000 $\text{h}^{-1}$	[35]	$S_{\text{BET}} = 23\text{--}30 \text{ m}^2 \text{ g}^{-1}$ , mixed phase
$x = 1.4$	Cu:Mn = 1:1, $\text{MnCl}_2$ , $\text{CuCl}_2$ , $\text{Na}_2\text{CO}_3$ , 3 h aging, 450 °C for 5 h	1000 ppm CO, GHSV = 50,000 $\text{mL g}^{-1} \text{ h}^{-1}$ , $T_{50}/T_{90} = 62/76$ °C, resp., reaction rate = 0.36 $\text{mmol g}^{-1} \text{ h}^{-1}$ and 1.45 $\text{mmol m}^{-2} \text{ h}^{-1}$ at 50 °C; reaction rates were measured at isotherm CO oxidation at 80–180 °C at less than 20% conversion	[13]	$S_{\text{BET}} = 18 \text{ m}^2 \text{ g}^{-1}$ , $V_p = 0.02 \text{ cm}^3 \text{ g}^{-1}$ , APD = 13
$x = 1.5$	Mn–acetate, Cu–nitrate, $\text{KMnO}_4$ , 300 °C for 2 h	1% CO (20% air in Ar) was fed into the reactor for the CO oxidation reaction, $T_{50}/T_{70}/T_{90} = 59/79/93$ °C, resp., the complete transformation was found at 100 °C, Co and Fe doping increases the efficiency	[41]	Mixed phases
$x = 1.5$	Copper and manganese acetates in 1/2 molar ratio in water, NaOH solution, 298 K, pH 11 300 °C for 2 h	1% CO, 20% $\text{O}_2$ and 79% $\text{N}_2$ as feed gas with a space velocity of 20,000 $\text{mL h}^{-1} \text{ g cat}^{-1}$ . The temperature was ramped at a rate of 1 °C $\text{min}^{-1}$ from 0 °C to the final temperature, $T_{50}/T_{100} = 72/110$ °C, resp.	[25]	$S_{\text{BET}} = 70 \text{ m}^2 \text{ g}^{-1}$ , $V_p = 0.36 \text{ cm}^3 \text{ g}^{-1}$
$x = 1.5$	Hydrothermal method, aq. Cu and Mn nitrates, citric acid, urea, $\text{KMnO}_4$ solution, $\text{Mn}(\text{NO}_3)_2/\text{KMnO}_4 = 1:2$ and urea/citric acid/ $\text{Mn}_{\text{all}}/\text{Cu} = 1.5:1.5:1:0\text{--}0.2$ ; Aq. ammonia (25 wt.%), pH = 6–7, 180 °C for 12 h, 350 °C in air for 4 h	1.6 vol% CO, 20.8 vol% $\text{O}_2$ , and 77.6 vol% $\text{N}_2$ , a space velocity of 30,000 $\text{mL} \cdot \text{g}^{-1} \cdot \text{h}^{-1}$ . It is active at room temperature. 100% CO oxidation was achieved at 65 °C	[32]	Mixed phase, $S_{\text{BET}} = 112\text{--}126 \text{ m}^2 \text{ g}^{-1}$ , 5.8–10.1 nm size

$S_{\text{BET}}$ —specific surface area;  $V_p$ —the total adsorption pore volume at  $P/P_0 = 0.995$ ; APD—average pore diameter; TOF—turnover frequency; GHSV—gas hourly space velocity.

Table 5. Copper manganese oxide spinel catalysts and their activity in NO oxidation reactions.

$\text{Cu}_x\text{Mn}_{3-x}\text{O}_4$	Precursors, Preparation Method, and Conditions	Catalyst Efficiency and Reaction Conditions	Ref.	Remarks
$x = 1.5$	Hydrothermal method, aq. Cu and Mn nitrates, citric acid, urea, $\text{KMnO}_4$ solution, $\text{Mn}(\text{NO}_3)_2/\text{KMnO}_4 = 1:2$ and urea/citric acid/ $\text{Mn}_{\text{all}}/\text{Cu} = 1.5:1.5:1:0\text{--}0.2$ ; aq. ammonia (25 wt.%), pH = 6–7, 180 °C for 12 h, 350 °C in air for 4 h.	5 vol% NO, 10 vol% CO, and 85 vol% He as diluents, GHSV 24,000 $\text{mL} \cdot \text{g}^{-1} \cdot \text{h}^{-1}$ . The 100% NO conversion and 100% $\text{N}_2$ selectivity were achieved at 275 °C	[32]	Mixed phase, $S_{\text{BET}} = 112\text{--}126 \text{ m}^2 \text{ g}^{-1}$ , 5.8–10.1 nm size

$S_{\text{BET}}$ —specific surface area; GHSV—gas hourly space velocity.

Table 6. Desulfurization with  $\text{Cu}_x\text{Mn}_{3-x}\text{O}_4$  catalysts.

$\text{Cu}_x\text{Mn}_{3-x}\text{O}_4$	Precursors, Preparation Method, and Conditions	Catalyst Efficiency and Reaction Conditions	Ref.	Remarks
$x = 1.15$	$\text{CuO}$ , $\text{MnO}_2$ , 5% graphite, 950 °C for 6 h	Atmospheric pressure, space velocity of 6000 $\text{h}^{-1}$ , 0.5 vol% $\text{H}_2\text{S}$ , 10 vol% $\text{H}_2$ , 15 vol% $\text{H}_2\text{O}(\text{v})$ , 5 vol% $\text{CO}_2$ , and 15 vol% CO, balance $\text{N}_2$ , 600 °C	[12]	Mixed oxide phase, porous, $V_p = 0.16 \text{ cm}^3 \text{ g}^{-1}$
$x = 1.47$	$\text{CuO}$ , $\text{MnO}_2$ , 5% graphite, 950 °C for 6 h	Atmospheric pressure, space velocity of 6000 $\text{h}^{-1}$ , 0.5 vol% $\text{H}_2\text{S}$ , 10 vol% $\text{H}_2$ , 15 vol% $\text{H}_2\text{O}(\text{v})$ , 5 vol% $\text{CO}_2$ , and 15 vol% CO, balance $\text{N}_2$ , 600 °C	[12]	Mixed oxide phase, porous, $V_p = 0.14 \text{ cm}^3 \text{ g}^{-1}$

$V_p$ —the total adsorption pore volume at  $P/P_0 = 0.995$ .

**Table 7.** Removal of chlorinated hydrocarbons from air in the presence of  $\text{Cu}_x\text{Mn}_{3-x}\text{O}_4$  catalysts.

$\text{Cu}_x\text{Mn}_{3-x}\text{O}_4$	Precursors, Preparation Method, and Conditions	Catalyst Efficiency and Reaction Conditions	Ref.	Remarks
$x = 1.5$	Tetramethylammonium hydroxide precipitating agent, aq. copper(II) and manganese(II) salt solution, dry air at 400 °C for 5 h	Decomposition of trichloroethylene in moist air by post-plasma catalysis, 300 °C, <i>GHSV</i> 60,000 mL g <sup>-1</sup> h <sup>-1</sup> , relative humidity (20 °C) 15%, initial TCE concentration 300 ppm, 50% CO <sub>2</sub> yield. <i>T</i> <sub>50</sub> = 300 °C (244 °C for CO <sub>2</sub> formation).	[48]	SiC support, <i>S</i> <sub>BET</sub> = 30 m <sup>2</sup> g <sup>-1</sup> , <i>V</i> <sub>p</sub> = 0.29 cm <sup>3</sup> g <sup>-1</sup>

*S*<sub>BET</sub>—specific surface area; *V*<sub>p</sub>—the total adsorption pore volume at *P*/*P*<sub>0</sub> = 0.995; *GHSV*—gas hourly space velocity.

**Table 8.** Removal of benzene from the air in the presence of  $\text{Cu}_x\text{Mn}_{3-x}\text{O}_4$  catalysts.

$\text{Cu}_x\text{Mn}_{3-x}\text{O}_4$	Precursors, Preparation Method, and Conditions	Catalyst Efficiency and Reaction Conditions	Refs.	Remarks
$x = 0.5$	Citric acid monohydrate, copper nitrate and 50% manganese nitrate solutions, ethylene glycol, 70 °C, the gel was dried and calcined for 3 h at 500 °C	100 ppm benzene in synthetic air, <i>GHSV</i> = 60,000 mL g <sup>-1</sup> h <sup>-1</sup> , <i>T</i> <sub>10</sub> / <i>T</i> <sub>50</sub> / <i>T</i> <sub>90</sub> = 114/164/193 °C, resp.	[46]	Crystallite size 13.2 nm, <i>S</i> <sub>BET</sub> = 45.00 m <sup>2</sup> g <sup>-1</sup> , <i>V</i> <sub>p</sub> = 0.310 cm <sup>3</sup> g <sup>-1</sup>
$x = 1.0$	Mn and Cu nitrate, NaHCO <sub>3</sub> as precipitating agent, 400–600 °C	150 ppm benzene concentration, 10% O <sub>2</sub> in the gas stream, 2250 ppm ozone, 70 °C	[42]	Mixture with oxide phases
$x = 1.0$	Citric acid monohydrate, copper nitrate and 50% manganese nitrate solutions, ethylene glycol, 70 °C, the gel was dried and calcined for 3 h at 500 °C	100 ppm benzene in synthetic air, <i>GHSV</i> = 60,000 mL g <sup>-1</sup> h <sup>-1</sup> , <i>T</i> <sub>10</sub> / <i>T</i> <sub>50</sub> / <i>T</i> <sub>90</sub> = 96/149/186 °C, resp.	[46]	Crystallite size 11.6 nm, <i>S</i> <sub>BET</sub> = 68.26 m <sup>2</sup> g <sup>-1</sup> , <i>V</i> <sub>p</sub> = 0.314 cm <sup>3</sup> g <sup>-1</sup>
$x = 1.5$	Citric acid monohydrate, copper nitrate and 50% manganese nitrate solutions, ethylene glycol, 70 °C, the gel was dried and calcined for 3 h at 500 °C	100 ppm benzene in synthetic air, <i>GHSV</i> = 60,000 mL g <sup>-1</sup> h <sup>-1</sup> , <i>T</i> <sub>10</sub> / <i>T</i> <sub>50</sub> / <i>T</i> <sub>90</sub> = 136/188/216 °C, resp.	[46]	Crystallite size 14.7 nm, <i>S</i> <sub>BET</sub> = 26.53 m <sup>2</sup> g <sup>-1</sup> , <i>V</i> <sub>p</sub> = 0.161 cm <sup>3</sup> g <sup>-1</sup>
$x = 2$	Citric acid monohydrate, copper nitrate and 50% manganese nitrate solutions, ethylene glycol, 70 °C, the gel was dried and calcined for 3 h at 500 °C	100 ppm benzene in synthetic air, <i>WHSV</i> = 60,000 mL g <sup>-1</sup> h <sup>-1</sup> , <i>T</i> <sub>10</sub> / <i>T</i> <sub>50</sub> / <i>T</i> <sub>90</sub> = 149/198/220 °C, resp.	[46]	Crystallite size 18.3 nm, <i>S</i> <sub>BET</sub> = 25.44 m <sup>2</sup> g <sup>-1</sup> , <i>V</i> <sub>p</sub> = 0.177 cm <sup>3</sup> g <sup>-1</sup>

*S*<sub>BET</sub>—specific surface area; *V*<sub>p</sub>—the total adsorption pore volume at *P*/*P*<sub>0</sub> = 0.995; *GHSV*—gas hourly space velocity.

#### 4.1. Removal of Carbon Monoxide from the Air

The Hopcalite catalyst used for the removal of CO from air is a mixed copper manganese oxide, the composition of which strongly depends on the synthesis conditions. Hopcalite was developed by the USA Chemical Warfare Service for gas masks against carbon monoxide during World War I. The heat treatment history of the Hopcalite catalyst is a key factor to ensure its catalytic activity in CO removal at room temperature [33,45]. The samples prepared between 400 and 500 °C for a calcination time of 2–18 h resulted in catalysts containing  $\text{CuMn}_2\text{O}_4$ , but their activity dropped to zero if the sample was prepared at 500 °C in 18 h. The sample containing crystalline  $\text{CuMn}_2\text{O}_4$  was active for the room temperature oxidation of CO, but the amorphous precursors prepared by calcination at 300 °C showed higher activity than  $\text{CuMn}_2\text{O}_4$  [33].

The lowest Cu content ( $x = 0.5$ ) among the studied  $\text{Cu}_x\text{Mn}_{3-x}\text{O}_4$  catalysts proved to be active in CO oxidation was found in the samples prepared by the heat treatment of basic

copper(II) permanganate,  $\text{Cu}_2(\text{OH})_3\text{MnO}_4$ . This catalyst was active for CO removal at 30 °C [55]. The catalyst with the same composition prepared by precipitation from copper and manganese nitrates solution with NaOH and heated at 300 °C reached quantitative CO conversion in air at 120 °C [25].

The  $\text{CuMn}_2\text{O}_4$  catalysts with  $x = 1$ , which are active in CO oxidation reactions, were prepared in various reaction routes (Table 4), including precipitation from metal nitrates with  $\text{Na}_2\text{CO}_3$  [33,35], via the formation of complexes with citric acid and ethylene glycol (oxalate precursor) [39], and by the thermal decomposition of  $[\text{Cu}(\text{NH}_3)_4](\text{MnO}_4)_2$  in  $\text{CHCl}_3$  and  $\text{CCl}_4$  at 61 and 77 °C [60]. The thermal decomposition of  $[\text{Cu}(\text{NH}_3)_4](\text{MnO}_4)_2$  under inert solvents resulted in nanosized  $\text{CuMn}_2\text{O}_4$  with a defect structure. The best catalytic performance in CO oxidation was found for the catalysts prepared in  $\text{CHCl}_3$  and  $\text{CCl}_4$  with the aqueous extraction of the  $\text{NH}_4\text{NO}_3$  intermediate with subsequent annealing at 300 °C for 1 h (80 and ~95%, respectively). If the ammonium nitrate was removed by thermal decomposition, the catalytic activity of the Cu–Mn spinels in the course of CO oxidation [60] decreased. A catalyst ( $\text{CCl}_4$ , aq. leaching, 300 °C) was tested in 5 cycles (each cycle was 22–25 h). Its catalytic activity decreased with increasing reaction time from  $5 \times 10^{-3}$  to  $2.5 \times 10^{-3}$  mol  $\text{CO}_2$   $\text{m}^{-2}$   $\text{h}^{-1}$  at 125 °C, mainly in the first three hours. This kind of activity profile was found for commercial Hopcalite catalysts as well [75].

Mixed-phase  $\text{Cu}_x\text{Mn}_{3-x}\text{O}_4$  spinel catalysts containing  $\text{Mn}_2\text{O}_3$  were developed for fuel cells PROX (preferential CO oxidation in CO +  $\text{H}_2$  mixtures). Copper and manganese nitrates were refluxed in a mixture of ethylene glycol, water, and concentrated nitric acid for 2 h and dried at 105 °C for an additional 16 h followed by calcination at a temperature of 350 and 500 °C for 5 h. The obtained samples converted 20 and 17% CO in 1 h at room temperature, respectively [39].

The precipitation method using  $\text{Na}_2\text{CO}_3$  and metal nitrates resulted in Cu–Mn spinels with  $x = 1.0$ – $1.4$ , depending on the aging time (from 0 to 1440 min). The conversion of CO was found to be ca. 50% for the unaged catalyst at room temperature and decreased with increasing aging time, but catalytic performance is restored after 720 min and reaches its maximum (the highest CO conversion). For this aging time, the composition of the catalyst is characterized by  $x = 1$  ( $\text{CuMn}_2\text{O}_4$ ) [35]. The copper-rich catalysts with  $x = 1.4$ – $1.5$  were prepared by precipitation methods, starting from the appropriate metal nitrates [35,41], acetates [25,41] and chlorides [13], by redox methods using  $\text{KMnO}_4$  [41] and by combined methods using  $\text{KMnO}_4$  and hydrothermal treatments with complex forming reagents, such as citric acid or oxalate precursors (ethylene glycol) [32]. Their detailed catalytic activities in CO oxidation are given in Table 4. The  $\text{Cu}_{1.5}\text{Mn}_{1.5}\text{O}_4$  catalysts synthesized by the co-precipitation method from acetate or nitrate salt solutions of copper and manganese with NaOH and  $\text{Na}_2\text{CO}_3$  were studied in detail [25] to maximize the efficiency of CO oxidation at room temperature. The activity of the oxidation of CO strongly depended on the combination of precipitant and precursor anions, ranking in the order (acetate + carbonate) > (nitrate + carbonate) > (acetate + hydroxide) > (nitrate + hydroxide) [25]. The redox reaction of Mn-acetate, Cu-nitrate, and  $\text{KMnO}_4$  solution with calcination of the reaction product in air at 300 °C for 2 h resulted in a catalyst with the same composition ( $\text{Cu}_{1.5}\text{Mn}_{1.5}\text{O}_4$ ), which was used in the low-temperature oxidation of CO. The presence of other transition metals added to the catalysts improved the catalytic properties. For example, the  $T_{50}$  temperatures of CO conversion were 34 and 50 °C with Co- and Fe-doping, respectively [41]. The catalyst was prepared with a hybrid method, with the use of  $\text{KMnO}_4$  as oxidant and citric acid as a complex-forming agent, together with ethylene glycol as oxalate precursor under hydrothermal conditions (180 °C for 12 h) and by calcination at 350 °C in air for 4 h contained nanosized (5–10 nm) particles [32]. The mechanism of the oxidation of CO with this catalyst is shown in Figure 4.

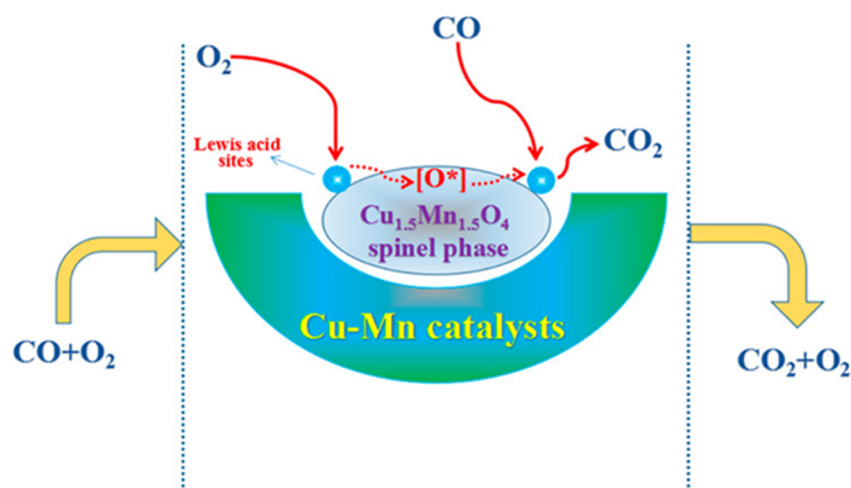


**Figure 4.** Mechanism of CO oxidation catalyzed by  $\text{Cu}_{1.5}\text{Mn}_{1.5}\text{O}_4$  prepared with a hybrid (redox, complex forming, and hydrothermal) method (reproduced from ref. [32]).

This catalyst shows activity even at room temperature, but 100% CO oxidation was achieved only at a temperature of 65 °C [32]. A plausible tentative mechanism for the carbon monoxide oxidation reaction over the copper manganese oxide spinel catalysts includes two main processes:

- (1) Molecular oxygen is preferentially adsorbed on the spinel surface and subsequently forms surface-active species containing adsorbed oxygen ( $\text{O}^*$ ) such as  $\text{O}_2^-$  (ads) and  $\text{O}^-$  (ads).
- (2) CO molecules are oxidized by  $\text{O}^*$  species with the formation of gaseous carbon dioxide. The two-step reaction can be formulated as e.g.,  $\text{CO} + \text{O}^-$  (ads)  $\rightarrow$   $\text{CO}_2 + \text{e}^-$  and  $\text{CO} + 2\text{O}^-$  (ads)  $\rightarrow$   $\text{CO}_3^{2-}$  (ads).

The cooperative effect of the redox cycle between the metal centers in the spinel catalyst ( $\text{Cu}^+ + \text{Mn}^{4+} \leftrightarrow \text{Cu}^{2+} + \text{Mn}^{3+}$ ) involving the  $\text{Cu}^{2+}$  and  $\text{Mn}^{3+}$  ions of the distorted spinel structure promotes the generation of Lewis acid sites on the surface, which play a beneficial role in the activation of reactants to form active species. These lead to the enhancement of catalytic activity (performance) in the CO oxidation reactions. The spinel catalyst transports the surface  $\text{O}^*$  species. The  $\text{Cu}^{2+}\text{-O-Mn}^{3+}$  units lose some oxygen to form  $\text{CO}_2$  from CO and form oxygen defects. The spinel phase captures some oxygen from the gas phase to form surface-active  $\text{O}^*$  species again. The detailed mechanism is given in [32].

#### 4.2. Removal of NO from Air by Carbon Monoxide

The reaction of NO with carbon monoxide in the presence of copper manganese oxide catalysts, especially  $\text{Cu}_{1.5}\text{Mn}_{1.5}$  spinels, results in  $\text{CO}_2$  and  $\text{N}_2$ . The aging time of samples prepared from metal nitrates with sodium carbonate has crucial importance in the preparation of a catalyst for the NO SCR with carbon monoxide at ambient temperature [35]. The  $\text{Cu}_{1.5}\text{Mn}_{1.5}\text{O}_4$  nanocatalyst given in Table 5 was prepared with a hybrid method. It can adsorb  $\text{NO}_x$  gases due to the presence of  $\text{Cu}^+\text{-CO}$  active species. The surface-dispersed  $\text{Cu}^{x+}\text{-O}_2^-\text{-Mn}^{y+}$  active species can be reduced to  $\text{Cu}^+\text{-}\square\text{-Mn}^{(4-x)+}$  active species at increasing adsorption temperature, and the synergetic effects between Cu and Mn ( $\text{Cu}^{x+}\text{-O}_2^-\text{-Mn}^{y+}$  species) also play a role in the NO + CO SCR reaction [16]. The mechanism of the reaction is shown in Figure 5.

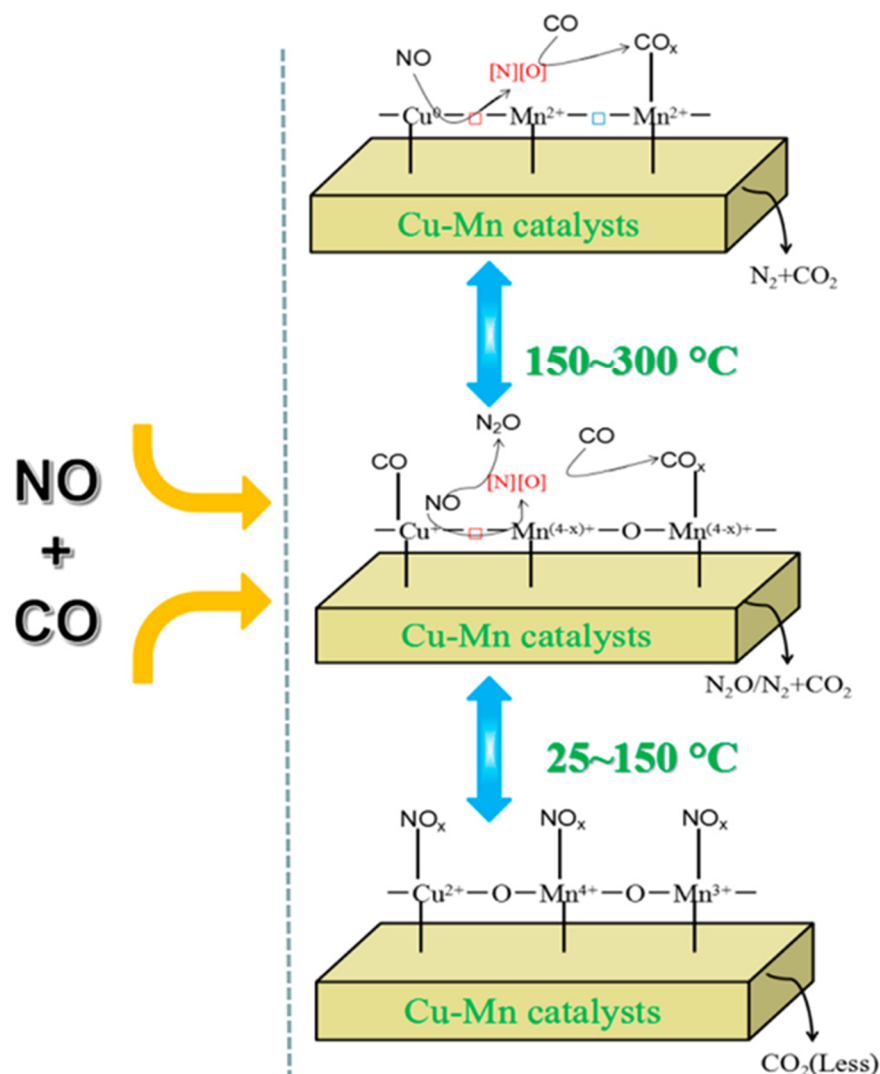


**Figure 5.** The mechanism of NO reduction with adsorbed CO on Cu–Mn–spinel catalysts (reproduced from [32]).

A possible tentative reaction mechanism for the NO + CO reaction over copper manganese oxide spinel catalysts (illustrated in Figure 5) is given in [32]. The formation of surface oxygen vacancies in the spinel catalysts contributes to the activation of NO and CO gases via the formation of highly reactive species. NO molecules are preferentially adsorbed on the spinel surface with the formation of surface NO<sub>x</sub> species, thus only a small part of carbon monoxide molecules is oxidized by surface active oxygen (O\*) derived from Cu–O–Mn linkages. The surface NO<sub>x</sub> species are gradually dissociated into N and O atoms, with the formation of N<sub>2</sub>O as an intermediate product [32], and surface O vacancies are also produced due to the synergistic effect between Cu and Mn.

The high or intermediate oxidation-state metal ions such as Mn<sup>4+</sup>, Mn<sup>3+</sup>, and Cu<sup>2+</sup> are partially reduced by carbon monoxide with the formation of low or intermediate valence metal species, such as Mn<sup>3+</sup>, Mn<sup>2+</sup>, Cu<sup>+</sup> or Cu<sup>0</sup>. The interaction between divalent and monovalent metal ions and surface CO<sub>x</sub> species forms Mn<sup>2+</sup>–CO<sub>x</sub> and Cu<sup>+</sup>–CO species. The higher the temperature, the more oxygen vacancies are generated, resulting in an enhancement of catalytic activity/performance. The catalytic cycle is when the CO molecules and the intermediate N<sub>2</sub>O turn into gaseous CO<sub>2</sub> and N<sub>2</sub>.

#### 4.3. Removal of Other Pollutants from the Air and Other Gases

Copper manganese spinel catalysts are widely used materials in the oxidative recovery of various other inorganic and organic pollutants such as H<sub>2</sub>S (Table 6), chlorinated hydrocarbons (Table 7), and aromatic hydrocarbons (Tables 8 and 9). The recovery of hydrogen sulfide with porous copper-rich Cu<sub>x</sub>Mn<sub>3-x</sub>O<sub>4</sub> spinel catalysts prepared from finely divided CuO, MnO<sub>2</sub>, and graphite ( $x = 1.47$  and  $x = 1.15$ ) were tested from hot coal gas in the presence and absence of water. The pores in the catalysts are produced due to the release of the CO<sub>2</sub> gas that formed from the graphite and oxide phases. The regeneration of catalysts was performed with a regeneration gas containing 3 vol% O<sub>2</sub> (balance N<sub>2</sub>) at 720 °C [12].

The oxidative removal of trichloroethylene from air was studied in the presence of Cu<sub>1.5</sub>Mn<sub>1.5</sub>O<sub>4</sub> catalyst carried out on SiC support. The decomposition of trichloroethylene in moist air (relative humidity was 15%) was done by post-plasma catalysis above 150 °C. Trichloroethylene removal is 19% and 50% at 250 °C and 300 °C, respectively. Up to 250 °C, the selectivity of the catalyst into CO<sub>2</sub> is 100%, whereas, at 300 °C, C<sub>2</sub>Cl<sub>4</sub>, CO, and CO<sub>2</sub> formed (Table 7) [58].

#### 4.4. Removal of Aromatic Hydrocarbons from Air

The strong carcinogen effect of benzene generated a demand to remove it from the air. This may be done in the presence of Cu<sub>x</sub>Mn<sub>3-x</sub>O<sub>4</sub> spinels with either synthetic air [46] or ozone [42]. The high reactivity of ozone towards benzene ensures a much lower reaction temperature (70 °C) than that of synthetic air (Table 8) [42,46]. The ozonation reaction was catalyzed with a mixed oxide phase containing CuMn<sub>2</sub>O<sub>4</sub> prepared from Mn and Cu–nitrate solutions with NaHCO<sub>3</sub>, by calcination between 400 and 600 °C. Oxidation with synthetic air was tested with a series of Cu<sub>x</sub>Mn<sub>3-x</sub>O<sub>4</sub> spinels with  $x = 0.5, 1.0, 1.5,$  and  $2$ . The Cu<sup>II</sup>/Cu<sup>I</sup> or Mn<sup>III</sup>/Mn<sup>IV</sup> ratios for the spinels with  $x = 0.5, 1.0, 1.5,$  and  $2.0$  were found to be 12.0, 20.6, 4.5, and 7.8 or 2.0, 2.5, 1.4, and 0.6, respectively. The catalytic oxidation of benzene was complete at a temperature lower than 200 °C. The Mn<sup>III</sup>-occupied octahedral positions of the spinel lattice greatly improve catalytic activity, and the surface lattice O-species play a key role in the process [46].

The removal of toluene from air in the presence of various Cu<sub>x</sub>Mn<sub>3-x</sub>O<sub>4</sub> spinels ( $x = 0.5$ – $1.5$ ) was studied in detail (Table 9). These catalysts were synthesized from the appropriate nitrate, acetate, and chloride salts by precipitation with hydroxides (NaOH [49], NH<sub>4</sub>OH [47], Me<sub>4</sub>NOH [26]) or carbonates (Na<sub>2</sub>CO<sub>3</sub> [13,26] or (NH<sub>4</sub>)<sub>2</sub>CO<sub>3</sub>) [37], including reverse emulsion formation [47] or hydrothermal reactions [49]. Incipient wetness impregnation and direct pyrolysis on  $\gamma$ -Al<sub>2</sub>O<sub>3</sub> [76] and anatase [18] were used to prepare supported catalysts. A series of TiO<sub>2</sub>-supported mixed-phase catalysts containing Cu<sub>1.4</sub>Mn<sub>1.6</sub>O<sub>4</sub> showed high catalytic activity with the total conversion (100%) of toluene into carbon dioxide above 240 °C, without any deactivation of the catalyst. The mobility of the network oxygen in the structure of the catalyst is a key factor in the catalytic process. The gradual loss of catalytic activity below 240 °C can be attributed to the adsorption of carbonaceous compounds on the surface, and according to this, catalytic activity can easily be regenerated by heating the used catalysts in airflow at 300 °C [18].

Alcoholic dehydration of the xerogel made with sodium alginate from Cu(II) and Mn(II) salt solutions resulted in cubic nanosized Cu<sub>1.5</sub>Mn<sub>1.5</sub>O<sub>4</sub> [38]. This nanosized cubic Cu<sub>1.5</sub>Mn<sub>1.5</sub>O<sub>4</sub> proved to be a high-performance catalyst in the oxidation of toluene at atmospheric pressure. The CuMn<sub>2</sub>O<sub>4</sub> prepared from copper acetate and manganese nitrate in reverse microemulsion (Triton-X-100 surfactant, n-octanol, and cyclohexane) by adding NH<sub>4</sub>OH and calcining at 450–1000 °C in oxygen also catalyzed toluene combustion (0.35% toluene and 9% O<sub>2</sub> in inert gas). The ignition temperature of 210 °C and a combustion temperature of 220 °C resulted in the complete oxidation of toluene [47]. The oxidation of toluene in the presence of this catalyst was complete at ~240 °C [38].

The catalyst containing stoichiometric CuMn<sub>2</sub>O<sub>4</sub>, which was prepared from nitrate salts with tetramethylammonium hydroxide, was active in toluene oxidation with the formation of CO<sub>2</sub> as the main product with 22 (10.45) and 1.9 (0.04)  $\mu\text{mol g}^{-1} \text{h}^{-1}$  ( $\mu\text{mol m}^{-2} \text{h}^{-1}$ ) de-

composition rate at 170 and 150 °C, respectively. Only a minor amount of benzene and CO formed [26]. Oxygen is adsorbed by the surface ( $O_{ads}$ ), but the subsurface oxygen content also plays a key role in the activity of the catalyst [26]. The rod-like nanosized (10–20 nm) copper manganese mixed oxides containing  $CuMn_2O_4$  were prepared from copper and manganese acetate with  $Na_2CO_3$  under hydrothermal conditions. These catalysts have significantly higher catalytic activity for toluene combustion at a temperature of 210 °C than that found for  $CuMn_2O_4$  prepared without hydrothermal post-treatment even at a combustion temperature of 250 °C [49]. It was attributed to the higher surface concentration of high valence ionic species such as  $Cu^{2+}$ ,  $Mn^{3+}$ , and  $Mn^{4+}$ , and surface oxygen concentration in the nanorods, than those in the  $CuMn_2O_4$  made without hydrothermal treatment [23]. The hydrothermal process increases the surface  $Mn^{4+}$  concentration up to 40% in the hydrothermally prepared nanorods due to the  $Cu^{2+} + Mn^{3+} \leftrightarrow 2 Cu^+ + Mn^{4+}$  [77]. The excess surface oxygen combines more easily with toluene molecules than the adsorbed oxygen on the catalyst surface [78]. The  $\pi$  bond of the aromatic ring interacts with  $Cu^{2+}$  with the formation of a transition complex, and the  $d$  electrons of  $Cu^{2+}$  can be fed back to the  $\pi$  bond system of the toluene molecule [34].

The catalytic activity of the copper-rich  $Cu_{1.5}Mn_{1.5}O_4$  spinels in toluene oxidation can be increased by La-loading [37]. Lanthanum acts as a structure promoter and increases the surface area and diminishes the crystallinity of the catalyst. As an electron promoter, lanthanum changes the valence state and redox properties of copper and manganese located at various spinel sites. The reducibility of the La-doped catalysts is significantly improved, and there was also a significant increase in the surface oxygen concentration [37].

**Table 9.** Removal of toluene from air in the presence of  $Cu_xMn_{3-x}O_4$  catalysts.

$Cu_xMn_{3-x}O_4$	Precursors, Preparation Method, and Conditions	Catalyst Efficiency and Reaction Conditions	Refs.	Remarks
$x = 1.0$	Cu-nitrate, Mn-acetate, Cu:Mn = 1:2, $\gamma$ - $Al_2O_3$ , 500 °C for 5 h	1000 ppm toluene in 7:3 $N_2:O_2$ , 120,000 $h^{-1}$ space velocity, $T_{50}/T_{90}$ = 369/474 °C, resp.	[76]	Supported on $Al_2O_3$ , $S_{BET} = \sim 101.3 \text{ m}^2 \text{ g}^{-1}$
$x = 1.0$	Cu and Mn(II) acetate, co-precipitation at 80 °C with aq. $Na_2CO_3$ , 500 °C	0.35% toluene and 9% $O_2$ in Ar, 250 °C	[49]	Mixed phase, $S_{BET} = 73 \text{ m}^2 \text{ g}^{-1}$
$x = 1.0$	Cu and Mn(II) acetate, hydrothermal treatment in 10 M NaOH at 110 °C for 20 h, 250 °C	0.35% toluene and 9% $O_2$ in Ar, GHSV 36,000, 210 °C; $T_{10}/T_{50}/T_{95}$ are 150, 170, 200 °C, resp.	[49]	Nanorods, mixed phase, $S_{BET} = 221 \text{ m}^2 \text{ g}^{-1}$
$x = 1.0$	Mn and Cu nitrates, co-precipitation with $Me_4NOH$ , 400 °C for 5 h	800 ppm toluene in air, 150 °C for 24 h, GHSV = 27,800 $\text{mL g}^{-1} \text{ h}^{-1}$ , $T_{10}/T_{50}/T_{90}$ = 185/195/200 °C, resp.	[26]	$S_{BET} = 48 \text{ m}^2 \text{ g}^{-1}$ , $V_p = 0.30 \text{ cm}^3 \text{ g}^{-1}$
$x = 1.2$	Cu-nitrate, Mn-acetate, Cu:Mn = 1:0.5, $\gamma$ - $Al_2O_3$ , 500 °C for 5 h	1000 ppm toluene in 7:3 $N_2:O_2$ , 120,000 $h^{-1}$ space velocity, $T_{50}/T_{90}$ = 330/383 °C, resp.	[76]	Supported on $Al_2O_3$ , $S_{BET} = \sim 109.2 \text{ m}^2 \text{ g}^{-1}$
$x = 1.3$	Cu-nitrate, Mn-acetate, Cu:Mn = 1:1.5, $\gamma$ - $Al_2O_3$ , 500 °C for 5 h	1000 ppm toluene in 7:3 $N_2:O_2$ , 120,000 $h^{-1}$ space velocity, $T_{50}/T_{90}$ = 271–303/293–329 °C, resp., depending on loaded amount on $Al_2O_3$	[76]	Supported on $Al_2O_3$ , $S_{BET} = \sim 99.0 \text{ m}^2 \text{ g}^{-1}$ , TOF = 0.05–0.28
$x = 1.4$	Mn and Cu-nitrates, anatase, incipient wetness impregnation, 500 °C for 7 h in air	Atmospheric pressure, 500 ppm toluene in air, 150–300 °C, 5 h, GHSV 5000 $h^{-1}$	[18]	Mixed phase, $S_{BET} = 34\text{--}48 \text{ m}^2 \text{ g}^{-1}$ , supported on $TiO_2$
$x = 1.4$	Cu:Mn = 1:1, $MnCl_2$ , $CuCl_2$ , $Na_2CO_3$ , 450 °C for 5 h	500 ppm toluene in humid air, GHSV = 50,000 $\text{mL g}^{-1} \text{ h}^{-1}$ , $T_{50}/T_{90}$ = 265/280 °C, resp., reaction rate = 0.001 $\text{mmol g}^{-1} \text{ h}^{-1}$ and 0.005 $\text{mmol m}^{-2} \text{ h}^{-1}$ at 200 °C	[13]	$S_{BET} = 18 \text{ m}^2 \text{ g}^{-1}$ , $P_v = 0.02 \text{ cm}^3 \text{ g}^{-1}$ , APD = 13

Table 9. Cont.

$\text{Cu}_x\text{Mn}_{3-x}\text{O}_4$	Precursors, Preparation Method, and Conditions	Catalyst Efficiency and Reaction Conditions	Refs.	Remarks
$x = 1.5$	Cu–nitrate, Mn–acetate, Cu:Mn = 1:2, $\gamma\text{-Al}_2\text{O}_3$ , 500 °C for 5 h	1000 ppm toluene in 7:3 $\text{N}_2:\text{O}_2$ , 120,000 $\text{h}^{-1}$ space velocity, $T_{50}/T_{90}$ = 300/343 °C, resp.	[76]	Supported on $\text{Al}_2\text{O}_3$ $S_{\text{BET}} = \sim 107.4 \text{ m}^2 \text{ g}^{-1}$
$x = 1.5$	ionotropic sodium alginate, metal chlorides, alcoholic dehydration, and calcining the xerogel at 450 °C	Toluene in dry air, 1000 ppm, $GHSV = 46,000 \text{ mL g}^{-1} \text{ h}^{-1}$ , reaction rate = 1.03 $\text{mmol g}^{-1} \text{ h}^{-1}$ and 24.52 $\text{mmol m}^{-2} \text{ h}^{-1}$ at 200 °C	[38]	cubic, $\sim 10 \text{ nm}$ size, $S_{\text{BET}} = 42 \text{ m}^2 \text{ g}^{-1}$
$x = 1.5$	Mn–acetate, Cu–nitrate, 1.5 M ammonium carbonate, pH = 8, 2 h, calcining at 550 °C for 2 h in air	1000 ppm toluene in air, $GHSV$ 30,000 $\text{h}^{-1}$ , $T_{50}/T_{90}$ = 245/274 °C, resp.	[37]	Mixed phase, undoped, $S_{\text{BET}} = 784.1 \text{ m}^2 \text{ g}^{-1}$ , $V_p$ (meso) = 0.246 and $V_p$ (all) 0.25 $\text{cm}^3 \text{ g}^{-1}$
$x = 1.5$	Mn–acetate, Cu–nitrate, La–nitrate, 1.5 M ammonium carbonate, pH = 8, 2 h, calcining at 550 °C for 2 h in air	1000 ppm toluene in air, $GHSV$ 30,000 $\text{h}^{-1}$ . $T_{50}/T_{90}$ for 2, 4, and 6% La content were 218/268, 217/255, and $-/280$ °C, respectively.	[37]	Mixed phase, 4% La-doping, $S_{\text{BET}} = 164.2 \text{ m}^2 \text{ g}^{-1}$ , $V_p$ (meso) 0.426 and $V_p$ (all) 0.45 $\text{cm}^3 \text{ g}^{-1}$

$S_{\text{BET}}$ —specific surface area;  $P_v$ —the total adsorption pore volume at  $P/P_0 = 0.995$ ;  $APD$ —average pore diameter;  $TOF$ —turnover frequency;  $GHSV$ —gas hourly space velocity.

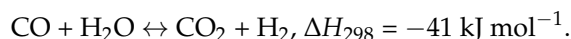
The  $\text{Cu}_{1.4}\text{Mn}_{1.6}\text{O}_4$  spinel catalyst showed activity in the combustion of benzene, toluene, and xylene. The acidity of the catalyst used in the oxidation of toluene decreased from ca. 89% to 79% after 2500 min, and the surface concentrations of  $\text{Cu}^{\text{II}}$  and  $\text{Mn}^{\text{IV}}$  were 56.8 and 56.9%. Catalytic activity decreased when  $\text{H}_2\text{O}$ ,  $\text{CO}_2$ , and  $\text{SO}_2$  were added, due to the formation of surface species. However, the deactivation is reversible. The aromatic hydrocarbons were oxidized into carbon dioxide, and only a minor amount of CO was detected as a consequence of the incomplete conversion of CO into  $\text{CO}_2$ . This means the catalyst is less efficient in the oxidation of CO than in the combustion of aromatic hydrocarbons [13].

## 5. Copper Manganese Oxides as Catalysts in Industrial Production Processes

Hydrogen gas is an essential raw material for numerous industrial processes, including ammonia and fertilizer synthesis and fine chemical industry, therefore converting the carbon monoxide content of water gas into carbon dioxide and hydrogen, and the methanol steam reforming processes have a huge importance. These processes can be catalyzed with copper manganese oxide spinels [20,36,40]. The hydrogen-rich  $\text{CO}:\text{H}_2$  mixtures (e.g., synthesis gas), however, resulted in the formation of important organic intermediates such as methyl formate in the presence of these copper–manganese oxide catalysts and the alkanol–DMF organic solvents [29,30].

### 5.1. Copper Manganese Oxide Spinel-Catalyzed Reactions of $\text{CO}:\text{H}_2$ Mixtures

The water–gas shift reaction is an enormously important industrial process for hydrogen generation through the conversion of CO gas produced by the steam reforming of hydrocarbons:



The catalytic performance of the catalysts containing  $\text{Cu}_{1.5}\text{Mn}_{1.5}\text{O}_4$ , which were prepared by the autoignition of copper and manganese nitrates with an excess of urea and by precipitation with sodium carbonate [36], was studied in the oxidative conversion of carbon monoxide (Table 10). The measured CO conversion strongly depended on the preparation method. The sample prepared by autoignition showed 90% conversion at 220 °C. The catalyst prepared by co-precipitation was less active in the 160–240 °C interval, and ca. 80% CO conversion was reached at 240 °C. The effect of space velocity on CO conversion over the catalyst prepared by the autoignition method was studied at 180 °C when a significant decrease of CO conversion by  $\sim 17$  and 32% was observed at  $GHSV = 6000$  and  $8000 \text{ h}^{-1}$ ,

respectively. The conversion CO at 180 °C increases when the partial pressure of water is increased from 5 to 10 kPa [26].

**Table 10.** The water–gas shift reaction in the presence of  $\text{Cu}_x\text{Mn}_{3-x}\text{O}_4$  catalysts.

$\text{Cu}_x\text{Mn}_{3-x}\text{O}_4$	Precursors, Preparation Method, and Conditions	Catalyst Efficiency and Reaction Conditions	Refs.	Remarks
1.5	Autoignition, 75% excess of urea, manganese nitrate, and copper, heating at 550 °C for 1 h	Space velocity = 4000 h <sup>-1</sup> , partial pressure of water vapor = 31.1 kPa, 4.492 vol.% CO/Ar + H <sub>2</sub> O and 15 vol.% CO, 10 vol.% CO <sub>2</sub> , 63 vol.% H <sub>2</sub> , 12 vol.% N <sub>2</sub> + H <sub>2</sub> O, CO conversion was 90% at 220 °C	[36]	Multiphase, $S_{\text{BET}} = 8.0 \text{ m}^2 \text{ g}^{-1}$
1.5	aqueous solutions of manganese and copper nitrate, Na <sub>2</sub> CO <sub>3</sub> at 80 °C, pH = 8.3, aging the resulting precipitate at 80 °C for 6 h, 700 °C for 7 h	Space velocity = 4000 h <sup>-1</sup> , partial pressure of water vapor = 31.1 kPa, 4.492 vol.% CO/Ar + H <sub>2</sub> O and 15 vol.% CO, 10 vol.% CO <sub>2</sub> , 63 vol.% H <sub>2</sub> , 12 vol.% N <sub>2</sub> + H <sub>2</sub> O, 160–240 °C, CO conversion was 80% at 240 °C	[36]	Multiphase, $S_{\text{BET}} = 5.9 \text{ m}^2 \text{ g}^{-1}$

$S_{\text{BET}}$ —specific surface area.

### 5.2. Synthesis of Methyl Formate

The copper manganese spinels with  $x = 0.5$  prepared from manganese nitrate and [tetraamminecopper(II)] hydroxide solutions with subsequent calcination at 450, 550, and 650 °C were tested in the synthesis of methyl formate from synthesis gas at 160 °C in 30 min with the MeOH:DMF solvent [29,30] (Table 11).

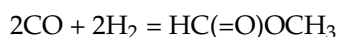


**Table 11.** Methyl formate synthesis from synthesis gas catalyzed by copper manganese oxide spinel containing catalysts.

$\text{Cu}_x\text{Mn}_{3-x}\text{O}_4$	Precursors, Preparation Method, and Conditions	Catalyst Efficiency and Reaction Conditions	Refs.	Remarks
$x = 1.5$	Mn(II)–nitrate:Cu(NH <sub>3</sub> ) <sub>4</sub> <sup>2+</sup> (Cu:Mn = 1:1), 35 °C, 550 °C for 4 h	MeOH–DMF as liquid phase, H <sub>2</sub> /CO = 2:1, 160 °C, 30 min	[30]	Mixed phase, $S_{\text{BET}} = 15 \text{ m}^2 \text{ g}^{-1}$ , $V_p = 0.03 \text{ cm}^3 \text{ g}^{-1}$ size is 38.4 nm
1.5	Mn(II)–nitrate:Cu(NH <sub>3</sub> ) <sub>4</sub> <sup>2+</sup> (Cu:Mn = 1:1), 35 °C, 550 °C for 4 h	CaO–ZrO <sub>2</sub> as co-catalyst, 1.5:3.5 (v/v) methanol–DMF as a solvent, 2:1 H <sub>2</sub> :CO molar ratio, room temperature up to 4.0 MPa, heating up to 160 °C in 1 h, stirring for 8 h; 12.7–16.6% CO conversion, $STY = 2.17\text{--}2.63 \text{ g L}^{-1} \text{ h}^{-1}$ , methyl formate selectivity was 81.3–83.6%	[29]	Mixed phase, $S_{\text{BET}} = 10.5\text{--}18.4 \text{ m}^2 \text{ g}^{-1}$ and $V_p = 0.02\text{--}0.04 \text{ cm}^3 \text{ g}^{-1}$ , nanosized sample

$S_{\text{BET}}$ —specific surface area;  $P_v$ —the total adsorption pore volume at  $P/P_0 = 0.995$ ;  $STY$ —space–time yield.

When the molar ratio of CO:H<sub>2</sub> was adjusted to 1:2, the selectivity of methyl formate formation (byproducts were CO<sub>2</sub>, EtOH, and formaldehyde) was >70% [30] whereas using a CaO–ZrO<sub>2</sub> co-catalyst resulted in an increase in selectivity up to >80% [30]. The best methyl formate space–time yield and selectivity, 4.19 g L<sup>-1</sup> h<sup>-1</sup> and 88.1%, respectively, were obtained on the spinel formed at 450 °C due to its high specific surface area. CO conversion in ethanol/DMF was higher than in methanol/DMF as solvent. The hydrogenation of methyl formate into methanol according to the equation



was catalyzed with the spinel prepared at 550 °C. Methyl formate showed high conversion (86.5%) with high methanol space–time yield and selectivity (Table 11) [30].

### 5.3. Methanol Steam Reforming Process

The steam reforming of methanol is a reaction that produces high H<sub>2</sub> yield/per mole methanol:



A series of Cu<sub>x</sub>Mn<sub>3-x</sub>O<sub>4</sub> catalysts with  $x = 0.3$ – $1.05$  prepared by the urea–nitrate combustion method at 550 °C were tested in the methanol steam reforming reaction under atmospheric pressure. Dilute (5% MeOH and 7.5% H<sub>2</sub>O) gas stream was used, and quantitative methanol conversion was achieved at 280 °C with the copper manganese oxide spinel catalysts with  $x = 0.6$ – $1.05$ . The superior catalysts resulted in H<sub>2</sub> and CO<sub>2</sub> between 240 and 280 °C, and only a small amount of CO was formed (CO and H<sub>2</sub> selectivity were between 1.7–6.4 and 91.9–97.5%, respectively, depending on the value of  $x$  and the reaction temperature [40] (Table 12).

**Table 12.** Steam reforming of methanol in the presence of catalysts containing copper manganese oxide spinel.

Cu <sub>x</sub> Mn <sub>3-x</sub> O <sub>4</sub>	Precursors, Preparation Method, and Conditions	Catalyst Efficiency and Reaction Conditions	Refs.	Remarks
$x = 0.3$	Combustion method, 50% excess of urea, Cu, and Mn–nitrate (4–500 °C), heat treatment at 550 °C for 1 h	Atmospheric pressure, 240–280 °C, $W/F = 0.257 \text{ g s}^{-1} \text{ cm}^{-3}$ , 5% MeOH, 7.5% H <sub>2</sub> O and He; 61/97% MeOH conversion, 1.7/5.4% CO and 96.3/94.6% H <sub>2</sub> selectivity, at 240 and 280 °C, resp.	[40]	$S_{\text{BET}} = 4.1 \text{ m}^2 \text{ g}^{-1}$
$x = 0.6$	Combustion method, 50% excess of urea, Cu, and Mn–nitrate (4–500 °C), heat treatment at 550 °C for 1 h	Atmospheric pressure, 240–280 °C, $W/F = 0.257 \text{ g s}^{-1} \text{ cm}^{-3}$ , 5% MeOH, 7.5% H <sub>2</sub> O and He; 83.6/100% MeOH conversion, 2.1/5.7% CO and 96.5/94.3% H <sub>2</sub> selectivity, at 240 and 280 °C, resp.	[40]	$S_{\text{BET}} = 7.5 \text{ m}^2 \text{ g}^{-1}$
$x = 0.75$	combustion method, 50% excess of urea, Cu, and Mn–nitrate (4–500 °C), heat treatment at 550 °C for 1 h	Atmospheric pressure, 240–280 °C, $W/F = 0.257 \text{ g s}^{-1} \text{ cm}^{-3}$ , 5% MeOH, 7.5% H <sub>2</sub> O and He; 91.6/100% MeOH conversion, 1.7/6.4% CO and 97.5/93.6% H <sub>2</sub> selectivity, at 240 and 280 °C, resp.	[40]	$S_{\text{BET}} = 6.0 \text{ m}^2 \text{ g}^{-1}$
$x = 0.9$	Combustion method, 50 % excess of urea, Cu, and Mn–nitrate (4–500 °C), heat treatment at 550 °C for 1 h	Atmospheric pressure, 240–280 °C, $W/F = 0.257 \text{ g s}^{-1} \text{ cm}^{-3}$ , 5% MeOH, 7.5% H <sub>2</sub> O and He; 93.1/100% MeOH conversion, 2.1/7.5% CO and 92.5/97.9% H <sub>2</sub> selectivity, at 240 and 280 °C, resp.	[40]	$S_{\text{BET}} = 4.8\text{--}8.6 \text{ m}^2 \text{ g}^{-1}$
$x = 1.05$	Combustion method, 50% excess of urea, Cu, and Mn–nitrate (4–500 °C), heat treatment at 550 °C for 1 h	Atmospheric pressure, 240–280 °C, $W/F = 0.257 \text{ g s}^{-1} \text{ cm}^{-3}$ , 5% MeOH, 7.5% H <sub>2</sub> O and He; 93.8/100% MeOH conversion, 2.1/9.1% CO and 91.9/97.9% H <sub>2</sub> selectivity, at 240 and 280 °C, resp.	[40]	$S_{\text{BET}} = 6.2 \text{ m}^2 \text{ g}^{-1}$
$x = 1.5$	1.2 M aqueous solution of Na <sub>2</sub> CO <sub>3</sub> , Cu, and Mn nitrates (each 0.5 M), pH at 8.5, 300 °C in air for 4 h	Atmospheric pressure, premixed water, and methanol with an H <sub>2</sub> O/MeOH molar ratio of 1.3; 51.5/65.7% MeOH conversion, 1.2/1.1 CO, and 99.6/99.1. H <sub>2</sub> selectivity at 240 and 260 °C, 246 and 157 mmol g <sub>cat</sub> <sup>-1</sup> h <sup>-1</sup> production rate, resp.	[20]	$S_{\text{BET}} = 55.2 \text{ m}^2 \text{ g}^{-1}$ , $V_p = 0.14 \text{ cm}^3 \text{ g}^{-1}$ , $d_p = 8.5$

Table 12. Cont.

$\text{Cu}_x\text{Mn}_{3-x}\text{O}_4$	Precursors, Preparation Method, and Conditions	Catalyst Efficiency and Reaction Conditions	Refs.	Remarks
$x = 1.5$	1.2 M aqueous solution of $\text{Na}_2\text{CO}_3$ , Cu and Mn nitrates (each 0.5 M), pH = 8.5, 500 °C in air for 4 h	Atmospheric pressure, premixed water, and methanol with an $\text{H}_2\text{O}/\text{MeOH}$ molar ratio of 1.3; 45.5/62% MeOH conversion, 1.7/1.5 CO, and 99.4/99.1 $\text{H}_2$ selectivity at 240 and 260 °C, with 139 and 189 $\text{mmol g}_{\text{cat}}^{-1} \text{h}^{-1}$ production rate, resp.	[20]	$S_{\text{BET}} = 14.9 \text{ m}^2 \text{ g}^{-1}$ , $V_{\text{p}} = 0.07 \text{ cm}^3 \text{ g}^{-1}$ , $d_{\text{p}} = 18.5 \text{ nm}$
$x = 1.5$	Aq. copper and manganese nitrate solution, 20% excess of oxalic acid at room temperature, 300 °C for 4 h	Atmospheric pressure, premixed water, and methanol with an $\text{H}_2\text{O}/\text{MeOH}$ molar ratio of 1.3; 43/60% MeOH conversion, 1.5/1.4% CO and 99.1–99.1% $\text{H}_2$ selectivity at 240 and 260 °C, with 131 and 182 $\text{mmol g}_{\text{cat}}^{-1} \text{h}^{-1}$ production rate, resp.	[20]	$S_{\text{BET}} = 9.6 \text{ m}^2 \text{ g}^{-1}$ , $V_{\text{p}} = 0.06 \text{ cm}^3 \text{ g}^{-1}$ , $d_{\text{p}} = 18.2 \text{ nm}$
$x = 1.5$	Aq. copper and manganese nitrate solution, 20% excess of oxalic acid at room temperature, 500 C for 4 h	Atmospheric pressure, premixed water, and methanol with an $\text{H}_2\text{O}/\text{MeOH}$ molar ratio of 1.3; 35/52.5% MeOH conversion, 1.5/1.5% CO and 99.1/99.4% $\text{H}_2$ selectivity at 240 and 260 °C, with 106 and 160 $\text{mmol g}_{\text{cat}}^{-1} \text{h}^{-1}$ production rate, resp.	[20]	$S_{\text{BET}} = 4.7 \text{ m}^2 \text{ g}^{-1}$ , $V_{\text{p}} = 0.05 \text{ cm}^3 \text{ g}^{-1}$ , $d_{\text{p}} = 35.6 \text{ nm}$
$x = 1.5$	A 1:2 molar ratio amount of $\text{Cu}_2\text{CO}_3(\text{OH})_2$ and $\text{MnCO}_3$ , 20% stoichiometric excess of solid oxalic acid dihydrate, grinding under ambient conditions in a planetary mill at a speed of 600 rpm for 2 h, 300 °C in air for 4 h	Atmospheric pressure, premixed water, and methanol with an $\text{H}_2\text{O}/\text{MeOH}$ molar ratio of 1.3; 74/88.5% MeOH conversion, 0.8/0.8% CO and 99–4/99.4 $\text{H}_2$ selectivity at 240 and 260 °C, with 226 and 170 $\text{mmol g}_{\text{cat}}^{-1} \text{h}^{-1}$ production rate, resp.	[20]	$S_{\text{BET}} = 96.1 \text{ m}^2 \text{ g}^{-1}$ , $V_{\text{p}} = 0.35 \text{ cm}^3 \text{ g}^{-1}$ , $d_{\text{p}} = 12.5 \text{ nm}$
$x = 1.5$	A 1:2 molar ratio amount of $\text{Cu}_2\text{CO}_3(\text{OH})_2$ and $\text{MnCO}_3$ , 20% stoichiometric excess of solid oxalic acid dihydrate, grinding under ambient conditions in a planetary mill at a speed of 600 rpm for 2 h, 500 °C in air for 4 h	Atmospheric pressure, premixed water, and methanol with an $\text{H}_2\text{O}/\text{MeOH}$ molar ratio of 1.3; 65/80.5% MeOH conversion, 1.3/1.5 CO, and 99.1/99.4% $\text{H}_2$ selectivity at 240 and 260 °C, with 199 and 246 $\text{mmol g}_{\text{cat}}^{-1} \text{h}^{-1}$ production rate, resp.	[20]	$S_{\text{BET}} = 24.6 \text{ m}^2 \text{ g}^{-1}$ , $V_{\text{p}} = 0.18 \text{ cm}^3 \text{ g}^{-1}$ , $d_{\text{p}} = 26.5 \text{ nm}$
$x = 1.5$	A 1:2 molar ratio amount of $\text{Cu}_2\text{CO}_3(\text{OH})_2$ and $\text{MnCO}_3$ premixed with 20% stoichiometric excess of solid oxalic acid, grinding under ambient conditions in a planetary mill at a speed of 600 rpm for 2 h with higher intensity (more balls), calcination at 300 °C in air for 4 h.	Atmospheric pressure, premixed water, and methanol with an $\text{H}_2\text{O}/\text{MeOH}$ molar ratio of 1.3; 79.9/92.9% MeOH conversion, 0.7/0.7% CO and 99.5/99.5% $\text{H}_2$ selectivity at 240 and 260 °C, with 244 and 284 $\text{mmol g}_{\text{cat}}^{-1} \text{h}^{-1}$ production rate, resp.	[20]	$S_{\text{BET}} = 118.1 \text{ m}^2 \text{ g}^{-1}$ , $V_{\text{p}} = 0.39 \text{ cm}^3 \text{ g}^{-1}$ , $d_{\text{p}} = 11.1 \text{ nm}$

Table 12. Cont.

$\text{Cu}_x\text{Mn}_{3-x}\text{O}_4$	Precursors, Preparation Method, and Conditions	Catalyst Efficiency and Reaction Conditions	Refs.	Remarks
$x = 1.5$	A 1:2 molar ratio of $\text{Cu}_2\text{CO}_3(\text{OH})_2$ and $\text{MnCO}_3$ premixed with 20% stoichiometric excess of solid citric acid, grinding under ambient conditions in a planetary mill (600 rpm) for 2 h, 500 °C in air for 4 h	Atmospheric pressure, premixed water, and methanol with an $\text{H}_2\text{O}/\text{MeOH}$ molar ratio of 1.3; 57/69% MeOH conversion, 1.5/1.6% CO and 99.4/99.6% $\text{H}_2$ selectivity at 240 and 260 °C, with 173 and 209 $\text{mmol g}_{\text{cat}}^{-1} \text{h}^{-1}$ production rate, resp.	[20]	$S_{\text{BET}} = 60.6 \text{ m}^2 \text{ g}^{-1}$ , $V_{\text{p}} = 0.30 \text{ cm}^3 \text{ g}^{-1}$ , $d_{\text{p}} = 17.5 \text{ nm}$

$S_{\text{BET}}$ —specific surface area;  $P_{\text{v}}$ —the total adsorption pore volume at  $P/P_0 = 0.995$ ;  $d_{\text{p}}$ —pore diameter;  $W/F$ —space velocity.

The catalytic activities of nanostructured Cu–Mn spinel oxides prepared in various reactions including the mechanochemical reaction of solid oxalic acid and citric acid with basic copper carbonate and manganese carbonate with subsequent calcination at 300 and 500 °C) were compared in the steam reforming reaction of methanol (Table 12). The catalytic activity of the copper–manganese oxide spinels prepared by mechanochemical reaction routes strongly depended on the milling intensity and the chemical nature of the precursors. The  $\text{Cu}_{1.5}\text{Mn}_{1.5}\text{O}_4$  spinel prepared with solid oxalic acid was extremely active and converted more than 92% of methanol at temperatures of 240 and 260 °C. The spinel prepared from citric acid precursors with the same composition converted only 68% of methanol. The samples prepared at 300 °C had much higher catalytic activity than those calcined at 500 °C. The superior activity of the spinel prepared by grinding oxalic acid and calcining it at 300 °C was attributed to the generation of the active  $\text{Cu}_{1.5}\text{Mn}_{1.5}\text{O}_4$  spinel phase and the high surface area, which provides high component dispersion. The catalytic performance of the spinels obtained with the same stoichiometry by the conventional co-precipitation with aq.  $\text{Na}_2\text{CO}_3$  is much inferior to the samples prepared by the mechanochemical methods, due to the low surface areas and the presence of less of the active phase of  $\text{Cu}_{1.5}\text{Mn}_{1.5}\text{O}_4$  spinel [20].

#### 5.4. Other Industrial Processes Catalyzed by $\text{Cu}_x\text{Mn}_{3-x}\text{O}_4$ Spinel

The copper-rich catalysts containing  $\text{Cu}_{1.5}\text{Mn}_{1.5}\text{O}_4$  spinel prepared with the conventional precipitation technique with sodium carbonate from the appropriate metal acetates were tested in the oxidation of toluene into benzyl alcohol. The catalysts (heat-treated between 400 and 800 °C) proved to be effective in the oxidation of toluene with molecular oxygen without using any solvents and additives, combining the advantages of minimized separation difficulties and equipment corrosion [34]. The main products were benzyl alcohol, benzaldehyde, and benzoic acid. The conversion of toluene (~17%) was higher than that found in the presence of other copper or manganese-based bimetallic Cu–(Zn, Si, Zr, Cr) or Mn–(Co, Ce, Fe) catalysts under 1.0 MPa oxygen pressure at 190 °C for 2 h. The distributions of the oxidation products strongly depend on the phase composition (heat treatment temperature and molar ratio of Cu and Mn acetate). The highest conversion of toluene (21.6%) was found with the spinel prepared at a 1:1 Cu:Mn ratio and the sintering temperature of 700 °C [34]. The benzyl alcohol was formed in 30 min in a high amount but transformed gradually into benzoic acid in 180 min. The highest selectivity to benzoic acid was in the sample made at 600 °C [34,43] (Table 13).

**Table 13.** Other industrial-scale reactions catalyzed by  $\text{Cu}_x\text{Mn}_{3-x}\text{O}_4$  spinels.

$x$	Preparation Method, Precursors, and Conditions	Reaction, Catalyst Efficiency, Catalytic Reaction Conditions	Ref.	Remark
$x = 1$	Precipitation, Cu- and Mn-acetate, $\text{Na}_2\text{CO}_3$ , calcination at $700^\circ\text{C}$	Toluene conversion into benzyl alcohol, benzaldehyde, and benzoic acid, ~21.6% conversion at $190^\circ\text{C}$ and 1.0 MPa $\text{O}_2$ pressure, 2 h	[34]	Size is 37 nm
$x = 1-2$	1 M copper nitrate and 1 M manganese nitrate 2 M fuel (glycerol), 1 M NaCl, $150^\circ\text{C}$ for 12 h, combustion at $400-700^\circ\text{C}$ for 6 h, self-propagating reaction	Propylene conversion into propylene oxide, 2:2:5 propylene:oxygen:helium volume ratio, $250-300^\circ\text{C}$ , 1 atm, $\text{GHSV} = 20\,000\text{ h}^{-1}$ , 30–37% selectivity at 1–3–1.5% conversion	[43]	Multiphase, $S_{\text{BET}} = 6.2\text{ m}^2\text{ g}^{-1}$ , $P_d$ 39.4 nm
$x = 1.5$	Spray granulation of $\text{CuO}$ and $\text{Mn}_3\text{O}_4$ in a spouted bed system, calcining for 2 h at $1125^\circ\text{C}$	Chemical Looping with Oxygen Uncoupling in coal combustion with $\text{CO}_2$ capture, 50 h	[15]	Mixed phase, $S_{\text{BET}} = 1.0$ , porosity is 12.1–18.7%

$S_{\text{BET}}$ —specific surface area;  $P_v$ —the total adsorption pore volume at  $P/P_0 = 0.995$ ;  $P_d$ —pore diameter;  $\text{GHSV}$ —gas hourly space velocity.

A series of mixed-phase catalysts containing  $\text{Cu}_x\text{Mn}_{3-x}\text{O}_4$  ( $1 < x < 2$ ) doped with NaCl were tested in the propylene epoxidation reaction. The catalysts were prepared by combustion synthesis (self-propagating reaction) with the use of a variety of fuels such as glycerol, maleic acid, citric acid, or ethyl acetoacetate. The optimal propylene oxide selectivity of 30–37% was achieved at 1.3–1.5% propylene conversion using a catalyst prepared with glycerol at  $550^\circ\text{C}$  [43].

The total combustion of solid coals with inherent  $\text{CO}_2$  separation was performed with the Chemical Looping with Oxygen Uncoupling (CLOU) process performed in the presence of mixed-phase catalysts containing  $\text{Cu}_{1.5}\text{Mn}_{1.5}\text{O}_4$  as oxygen carriers. Full combustion was reached, but  $\text{CO}_2$  capture efficiencies depended on coal rank [15].

## 6. Characterization and Operando Techniques Used in the Studying of $\text{Cu}_x\text{Mn}_{3-x}\text{O}_4$ Spinel Catalysts

The phase characterization of  $\text{Cu}_x\text{Mn}_{3-x}\text{O}_4$  spinels was performed with powder and single-crystal XRD studies. Vibrational spectroscopy including IR, far-IR, and Raman methods was also used.

The surface of the catalysts was characterized by X-ray photoelectron spectroscopy (XPS), energy dispersive X-ray spectroscopy (EDX), scanning electron microscopy (SEM), and  $\text{N}_2$  BET. Porosity was also characterized with BET isotherms measurements. Temperature-programmed desorption of  $\text{O}_2$ ,  $\text{H}_2$ , and other gases used in the catalytic reactions ( $\text{CO}$ ,  $\text{NO}$ , etc.) was also used. The decomposition reaction routes were monitored with DSC, TG, and TG–MS methods with simultaneous characterization of the solid phase by XRD, XPS, IR, SEM, EDX, and transmission electron microscopy (TEM).

Operando methods used to monitor the changes in the catalysts and conversion of reactants were mainly IR and GC methods. In situ diffuse-reflectance FT-IR spectra (DRIFTS) of fine powdery catalysts were recorded in in situ chambers. The reaction/desorption studies were performed by heating the adsorbed species and obtaining DRIFTS spectra at various targets.

The catalytic tests with gases were performed in various kinds of flow reactors, at atmospheric and high-pressure conditions and various temperatures. The liquid oxidation reactions were performed in an autoclave by adjusting the temperature/pressure conditions. The conversions were monitored by LC–MS or GC–MS.

## 7. Conclusions

The preparation and catalytic activity of  $\text{Cu}_x\text{Mn}_{3-x}\text{O}_4$  spinels and multiphase materials containing  $\text{Cu}_x\text{Mn}_{3-x}\text{O}_4$  spinels in a wide variety of industrial and environmental

protection processes are reviewed. The great diversity of metal ion valences and distribution in the spinel lattice, and the relation of the preparation and annealing methods on the crystallinity, composition, and chemical state of phases and surface layers play an important role in the catalytic activity of the  $\text{Cu}_x\text{Mn}_{3-x}\text{O}_4$  spinels. The presence of amorphous materials, lattice distortions, and the number of oxygen and metal vacancies are key factors in their catalytic activity. These features of  $\text{Cu}_x\text{Mn}_{3-x}\text{O}_4$  spinels can be controlled by the synthesis conditions, including the reaction routes, Cu/Mn ratios, starting metal compound valences, counter-ions, reagents, metal compound concentrations, temperature, time, and a wide variety of other reaction and annealing conditions.

The properties and catalytic activities and performances of the catalyst prepared by traditional solid-phase and solution-phase precipitating reactions were compared with the properties of the catalyst prepared new and promising synthesis routes were developed. The low-temperature methods ( $<100\text{ }^\circ\text{C}$ ) based on a solvent-mediated thermal decomposition of [tetraamminecopper(II)] permanganate results in amorphous phases, which can be transformed into regular spinel or bixbyite-like copper manganese oxides with a defect structure. The size and crystallinity of the copper manganese oxides prepared in this reaction route can be controlled with annealing time and temperature, and nanosized catalysts can be prepared even at  $500\text{ }^\circ\text{C}$ . These kinds of catalysts have been tested only in CO oxidation reactions, yet their studying in other industrially important reactions promises exciting possibilities to increase the performance of copper manganese oxide spinel catalysts in these processes. This reaction to prepare spinel oxides can be made with co-crystals or solid solutions made with [tetraamminecopper(II)] permanganate and other analog salts with various divalent cations or anions containing metal (e.g., perrhenate). In this way, a wide variety of metal-doped copper manganese oxide spinels can be prepared, which gives an almost infinite possibility to change the properties of amorphous or partially crystalline nanosized catalysts.

These perspectives pose new challenges to defect and synergic engineering to enhance the oxygen replenishment capacity of the doped  $\text{CuMn}_2\text{O}_4$  phases and control the amount and distribution of copper and oxygen vacancies in the spinel lattice sites. Developing (multi)-doped copper–manganese oxide catalysts to increase their efficiency and selectivity in various reactions helps substitute expensive and hardly available noble metal catalysts.

**Author Contributions:** Conceptualization, L.K.; writing—original draft preparation, L.K.; writing—review and editing, K.A.B., V.M.P. and L.B.; visualization, L.B.; supervision, L.K. and V.M.P.; project administration, L.B.; funding acquisition, L.K. and K.A.B. All authors have read and agreed to the published version of the manuscript.

**Funding:** The research was supported by the European Union and the State of Hungary, co-financed by the European Regional Development Fund (VEKOP-2.3.2-16-2017-00013) (L.K.) and the ÚNKP-21-3 and 22-3 New National Excellence Program of the Ministry for Innovation and Technology from the source of the National Research, Development, and Innovation Fund (K.A.B.).

**Data Availability Statement:** Not applicable.

**Conflicts of Interest:** The authors declare no conflict of interest.

## References

1. Zhang, K.; Ding, H.; Pan, W.; Mu, X.; Qiu, K.; Ma, J.; Zhao, Y.; Song, J.; Zhang, Z. Research Progress of a Composite Metal Oxide Catalyst for VOC Degradation. *Environ. Sci. Technol.* **2022**, *56*, 9220–9236. [[CrossRef](#)] [[PubMed](#)]
2. Han, X.; Wang, L.; Ling, H.; Ge, Z.; Lin, X.; Dai, X.; Chen, H. Critical review of thermochemical energy storage systems based on cobalt, manganese, and copper oxides. *Renew. Sustain. Energy Rev.* **2022**, *158*, 112076. [[CrossRef](#)]
3. Tang, Y.; Zhang, H.; Chen, J.; Shen, Y.; Xiong, K.; Zhou, Y.; Li, X.; Hu, Y. Different Active Phases of  $\text{CuMnO}_x$  for Total Oxidation and Partial Oxidation. *Cailiao Daobao/Mater. Rep.* **2020**, *34*, 9028–9033.
4. Yuvaraj, S.; Selvan, R.K.; Lee, Y.S. An overview of  $\text{AB}_2\text{O}_4$ - and  $\text{A}_2\text{BO}_4$ -structured negative electrodes for advanced Li-ion batteries. *RSC Adv.* **2016**, *6*, 21448–21474. [[CrossRef](#)]
5. Gao, P.-X.; Shimpi, P.; Gao, H.; Liu, C.; Guo, Y.; Cai, W.; Liao, K.-T.; Wrobel, G.; Zhang, Z.; Ren, Z.; et al. Hierarchical assembly of multifunctional oxide-based composite nanostructures for energy and environmental applications. *Int. J. Mol. Sci.* **2012**, *13*, 7393–7423. [[CrossRef](#)]

6. Lamb, A.B.; Bray, W.C.; Frazer, J.C.W. The Removal of Carbon Monoxide from Air. *J. Ind. Eng. Chem.* **1920**, *12*, 213–221. [[CrossRef](#)]
7. Lu, H.F.; Kong, X.X.; Huang, H.F.; Zhou, Y.; Chen, Y.F. Cu–Mn–Ce Ternary Mixed–Oxide Catalysts for Catalytic Combustion of Toluene. *J. Environ. Sci.* **2015**, *32*, 102–107. [[CrossRef](#)]
8. Aguilera, D.A.; Perez, A.; Molina, P.; Moreno, S. Cu–Mn and Co–Mn Catalysts Synthesized from Hydrotalcites and Their Use in the Oxidation of VOCs. *Appl. Catal. B Environ.* **2011**, *104*, 144–150. [[CrossRef](#)]
9. Broemme, A.D.D.; Brabers, V.A.M. Preparation and properties of copper– and manganese-containing mixed. *Solid State Ion.* **1985**, *16*, 171–178. [[CrossRef](#)]
10. Martin, B.E.; Petric, A. Electrical properties of copper–manganese spinel solutions and their cation valence and cation distribution. *J. Phys. Chem. Solids* **2007**, *68*, 2262–2270. [[CrossRef](#)]
11. Múčka, V.; Silber, R. Decomposition of hydrogen peroxide on nickel–silver two–component catalyst. *Collect. Czech. Chem. Commun.* **1984**, *49*, 2222–2230. [[CrossRef](#)]
12. Garcia, E.; Palacios, J.M.; Alonso, L.; Moliner, R. Performance of Mn and Cu Mixed Oxides as Regenerable Sorbents for Hot Coal Gas Desulfurization. *Energy Fuels* **2000**, *14*, 1296–1303. [[CrossRef](#)]
13. Wang, Y.; Yang, D.; Li, S.; Zhang, L.; Zheng, G.; Guo, L. Layered copper manganese oxide for the efficient catalytic CO and VOCs oxidation. *Chem. Eng. J.* **2019**, *357*, 258–268. [[CrossRef](#)]
14. Kotai, L.; Gacs, I.; Sajo, I.E.; Sharma, P.K.; Banerji, K.K. Beliefs and Facts in Permanganate Chemistry—An Overview on the Synthesis and the Reactivity of Simple and Complex Permanganates. *Trends Inorg. Chem.* **2009**, *11*, 25–104. [[CrossRef](#)]
15. Adánez–Rubio, I.; Abad, A.; Gayán, P.; de Diego, L.F.; Adánez, J. CLOU process performance with a Cu–Mn oxygen carrier in the combustion of different types of coal with CO<sub>2</sub> capture. *Fuel* **2018**, *212*, 605–612. [[CrossRef](#)]
16. Shaheen, W.M.; Selim, M.M. Effect of thermal treatment on physicochemical properties of pure and mixed manganese carbonate and basic copper carbonate. *Thermochim. Acta* **1998**, *322*, 117–128. [[CrossRef](#)]
17. Aoki, I. Cation Distribution in CuMn<sub>2</sub>O<sub>4</sub>. *J. Phys. Soc. Japan* **1965**, *20*, 871. [[CrossRef](#)]
18. Vu, V.H.; Belkouch, J.; Ould–Dris, A.; Taouk, B. Catalytic oxidation of volatile organic compounds on manganese and copper oxides supported on titania. *AIChE. J.* **2008**, *54*, 1585–1591. [[CrossRef](#)]
19. Wang, Z.; Zhu, J.; Sun, P.; Zhang, P.; Zeng, Z.; Liang, S.; Zhu, X. Nanostructured Mn–Cu binary oxides for supercapacitor. *J. Alloys Compd.* **2014**, *598*, 166–170. [[CrossRef](#)]
20. Liu, Q.; Wang, L.-C.; Chen, M.; Liu, Y.-M.; Cao, Y.; He, H.-Y.; Fan, K.-N. Waste–free Soft Reactive Grinding Synthesis of High–Surface–Area Copper–Manganese Spinel Oxide Catalysts Highly Effective for Methanol Steam Reforming. *Catal. Lett.* **2008**, *121*, 144–150. [[CrossRef](#)]
21. Vandenberghe, R.E.; Robbrecht, G.G.; Brabers, V.A.M. On the stability of the cubic spinel structure in the system Cu–Mn–O. *Mater. Res. Bull.* **1973**, *8*, 571–580. [[CrossRef](#)]
22. Loginova, M.V.; Stogova, V.A.; Sheftel, I.T. Structural transformations and electrical conductivity of copper–manganese spinel. *Izv. Ak. Nauk SSSR Ser. Neorg. Mater.* **1971**, *1*, 120.
23. Beley, M.; Padel, L.; Bernier, J.C. Etudes et Proprietes des Composés Cu<sub>x</sub>Mn<sub>3–x</sub>O<sub>4</sub>. *Ann. Chim. Fr.* **1978**, *3*, 429–452.
24. Jarrige, J.; Mexmain, J. Préparation et stabilité des manganites de cuivre. *Bull. Soc. Chim. Fr.* **1976**, 405–409.
25. Cai, L.N.; Guo, Y.; Lu, A.H.; Branton, P.; Li, W.C. The choice of precipitant and precursor in the co–precipitation synthesis of copper manganese oxide for maximizing carbon monoxide oxidation. *J. Mol. Catal. A Chem.* **2012**, *360*, 35–41. [[CrossRef](#)]
26. Ye, Z.; Giraudon, J.-M.; Nuns, N.; Simon, P.; De Geyter, N.; Morent, R.; Lamonnier, J.-F. Influence of the preparation method on the activity of copper–manganese oxides for toluene total oxidation. *Appl. Catal. B Environ.* **2018**, *223*, 154–166. [[CrossRef](#)]
27. Kótai, L.; Horváth, T.; Szentmihályi, K.; Keszler, Á. Evidence for quasi–intramolecular acid–base reactions in solutions of transition metal ammine complexes. *Transit. Met. Chem.* **2000**, *25*, 293–294. [[CrossRef](#)]
28. Kótai, L.; Gács, I.; Kazinczy, B.; Sajo, I.E. Quasi–intramolecular acid–base reactions in aqueous solutions of metal–complexes of basic ligands I. Generalized theoretical considerations on the deammoniation of [ML<sub>m</sub>]<sub>n</sub> type ammonia complexes. *Transit. Met. Chem.* **2003**, *28*, 292–295. [[CrossRef](#)]
29. Zhao, H.; Fang, K.; Zhou, J.; Lin, M.; Sun, Y. Direct synthesis of methyl formate from syngas on Cu–Mn mixed oxide catalyst. *Int. J. Hydrog. Energy* **2016**, *41*, 8819–8828. [[CrossRef](#)]
30. Zhao, H.; Fang, K.; Dong, F.; Lin, M.; Sun, Y.; Tang, Z. Textual properties of Cu–Mn mixed oxides and application for methyl formate synthesis from syngas. *J. Ind. Eng. Chem.* **2017**, *54*, 117–125. [[CrossRef](#)]
31. Saravanakumar, B.; Lakshmi, S.M.; Ravi, G.; Ganesh, V.; Sakunthala, A.; Yuvakkumar, R. Electrochemical properties of rice–like copper manganese oxide (CuMn<sub>2</sub>O<sub>4</sub>) nanoparticles for pseudocapacitor applications. *J. Alloys Compd.* **2017**, *723*, 115–122. [[CrossRef](#)]
32. Liu, T.; Yao, Y.; Wei, L.; Shi, Z.; Han, L.; Yuan, H.; Li, B.; Dong, L.; Wang, F.; Sun, C. Preparation and Evaluation of Copper–Manganese Oxide as a High–Efficiency Catalyst for CO Oxidation and NO Reduction by CO. *J. Phys. Chem. C.* **2017**, *121*, 12757–12770. [[CrossRef](#)]
33. Jones, C.; Cole, K.J.; Taylor, S.H.; Crudace, M.J.; Hutchings, G.J. Copper manganese oxide catalysts for ambient temperature carbon monoxide oxidation: Effect of calcination on activity. *J. Mol. Catal. A Chem.* **2009**, *305*, 121–124. [[CrossRef](#)]
34. Li, X.; Xu, J.; Zhou, L.; Wang, F.; Gao, J.; Chen, C.; Ning, J.; Ma, H. Liquid–phase oxidation of toluene by molecular oxygen over copper manganese oxides. *Catal. Lett.* **2006**, *110*, 149–154. [[CrossRef](#)]

35. Mirzaei, A.A.; Shaterian, H.R.; Habibi, M.; Hutchings, G.J.; Taylor, S.H. Characterisation of copper–manganese oxide catalysts: Effect of precipitate aging upon the structure and morphology of precursors and catalysts. *Appl. Catal. A Gen.* **2003**, *253*, 499–508. [[CrossRef](#)]
36. Tabakova, T.; Idakiev, V.; Avgouropoulos, G.; Papavasiliou, J.; Manzoli, M.; Boccuzzi, F.; Ioannides, T. Highly active copper catalyst for low–temperature water–gas shift reaction prepared via a Cu–Mn spinel oxide precursor. *Appl. Catal. A Gen.* **2013**, *451*, 184–191. [[CrossRef](#)]
37. Pan, J.; Du, W.; Liu, Y.; Cheng, Y.; Yuan, S. Lanthanum–doped CuMn composite oxide catalysts for catalytic oxidation of toluene. *J. Rare Earths* **2019**, *37*, 602–608. [[CrossRef](#)]
38. Behar, S.; Gonzalez, P.; Agulhon, P.; Quignard, F.; Świerczyński, D. New synthesis of nanosized Cu–Mn spinels as efficient oxidation catalysts. *Catal. Today* **2012**, *189*, 35–41. [[CrossRef](#)]
39. Krämer, M.; Schmidt, T.; Stöwe, K.; Müller, F.; Natter, H.; Maier, W.F. Structural and catalytic aspects of sol–gel derived copper manganese oxides as low–temperature CO oxidation catalyst. *Appl. Catal. A Gen.* **2006**, *302*, 257–263. [[CrossRef](#)]
40. Papavasiliou, J.; Avgouropoulos, G.; Ioannides, T. Steam reforming of methanol over copper–manganese spinel oxide catalysts. *Catal. Commun.* **2005**, *6*, 497–501. [[CrossRef](#)]
41. Choi, K.-H.; Lee, D.-H.; Kim, H.-S.; Yoon, Y.-C.; Park, C.-S.; Kim, Y.H. Reaction Characteristics of Precious–Metal–Free Ternary Mn–Cu–M (M = Ce, Co, Cr, and Fe) Oxide Catalysts for Low–Temperature CO Oxidation. *Ind. Eng. Chem. Res.* **2016**, *55*, 4443–4450. [[CrossRef](#)]
42. Einaga, H.; Kiya, A.; Yoshioka, S.; Teraoka, Y. Catalytic properties of copper manganese mixed oxides prepared by co–precipitation using tetramethylammonium hydroxide. *Catal. Sci. Technol.* **2014**, *4*, 3713–3722. [[CrossRef](#)]
43. Seubsai, A.; Kahn, M.; Zohour, B.; Noon, D.; Charoenpanich, M.; Senka, S. Copper–Manganese Mixed Metal Oxide Catalysts for the Direct Epoxidation of Propylene by Molecular Oxygen. *Ind. Eng. Chem. Res.* **2015**, *54*, 2638–2645. [[CrossRef](#)]
44. Bayón, R.; Vicente, G.S.; Maffiotte, C.; Morales, Á. Characterization of copper–manganese–oxide thin films deposited by dip–coating. *Sol. Energy Mater. Sol. Cells* **2008**, *92*, 1211–1216. [[CrossRef](#)]
45. Hutchings, G.J.; Mirzaei, A.A.; Joyner, R.W.; Siddiqui, M.R.H.; Taylor, S.H. Effect of preparation conditions on the catalytic performance of copper manganese oxide catalysts for CO oxidation. *Appl. Catal. A Gen.* **1998**, *166*, 143–152. [[CrossRef](#)]
46. Zhang, M.; Li, W.; Wu, X.; Zhao, F.; Wang, D.; Zha, X.; Li, S.; Liu, H.; Chen, Y. Low–temperature catalytic oxidation of benzene over nanocrystalline Cu–Mn composite oxides by facile sol–gel synthesis. *New J. Chem.* **2020**, *44*, 2442–2451. [[CrossRef](#)]
47. Li, W.B.; Chu, W.B.; Zhuang, M.; Hua, J. Catalytic oxidation of toluene on Mn–containing mixed oxides prepared in reverse microemulsions. *Catal. Today* **2004**, *93–95*, 205–209. [[CrossRef](#)]
48. Veerapandian, S.K.P.; Ye, Z.; Giraudon, J.-M.; De Geyter, N.; Morent, R.; Lamonier, J.-F. Plasma-assisted Cu–Mn mixed oxide catalysts for trichloroethylene abatement in moist air. *J. Hazard. Mater.* **2019**, *379*, 120781. [[CrossRef](#)]
49. Li, W.B.; Liu, Z.X.; Liu, R.F.; Chen, J.L.; Xu, B.Q. Rod–like CuMnO<sub>x</sub> transformed from mixed oxide particles by alkaline hydrothermal treatment as a novel catalyst for catalytic combustion of toluene. *Phys. Chem. Chem. Phys.* **2016**, *18*, 22794–22798. [[CrossRef](#)]
50. Jarrige, J.; Mexmain, J. Propriétés du Manganite de Cuivre Cu<sub>1,5</sub>Mn<sub>1,5</sub>O<sub>4</sub>. *Bull. Soc. Chim. Fr.* **1980**, *9–10*, I-363–I-369.
51. Kótai, L.; Sajó, I.E.; Gács, I.; Sharma, P.K.; Banerji, K.K. Convenient Routes for the Preparation of Barium Permanganate and other Permanganate Salts. *Z. Anorg. Allg. Chem.* **2007**, *633*, 1257–1260. [[CrossRef](#)]
52. Elovich, S.Y.; Roginskii, S.Z.; Shmuk, E.I. Kinetics of the Thermal Decomposition of Solid Permanganates. *Izv. AN SSSR Otdel. Khim. Nauk.* **1950**, *5*, 469–474.
53. Galwey, A.K.; Fakiha, S.A.A.; Abd El-Salaam, K.M. A kinetic and mechanistic study of the thermal decomposition of copper(II) permanganate. *Thermochim. Acta* **1994**, *239*, 225–232. [[CrossRef](#)]
54. Ball, M.C.; Downen, P.; Galwey, A.K. Chemical and physical properties of the solid products of thermal decomposition of copper(II) and nickel(II) permanganates. *J. Mater. Chem.* **1997**, *7*, 315–318. [[CrossRef](#)]
55. Yamanaka, S. Anion exchange reactions in layer structured crystals. *Stud. Surf. Sci. Catal.* **1994**, *83*, 147–153.
56. Kótai, L.; Banerji, K.K.; Sajó, I.; Kristóf, J.; Sreedharm, B.; Holly, S.; Keresztury, G.; Rockenbauer, A. An Unprecedented-Type Intramolecular Redox Reaction of Solid [Tetraamminecopper(2+)] Bis (permanganate)([Cu(NH<sub>3</sub>)<sub>4</sub>](MnO<sub>4</sub>)<sub>2</sub>)—A Low-Temperature Synthesis of Copper Dimanganese Tetraoxide-Type (CuMn<sub>2</sub>O<sub>4</sub>) Nanocrystalline Catalyst Precursors. *Helv. Chim. Acta* **2002**, *85*, 2316–2327. [[CrossRef](#)]
57. Gorbunov, V.V.; Shmagin, L.F. On the combustion of salts of tetramine copper (II). *Fiz. Goreniya Vzriva* **1972**, *8*, 523–526.
58. Seferiadis, N.; Dubler, E.; Oswald, H.R. Structure of [tetraamminecopper(II)] dipermanganate. *Acta Cryst. Sect. C.* **1986**, *42*, 942–945. [[CrossRef](#)]
59. Kótai, L.; Németh, P.; Kocsis, T.; Sajó, I.E.; Pasinszki, T. A new route to synthesize controlled–size MMn<sub>2</sub>O<sub>4</sub>–type transition metal (M = Cd, Zn, Cu) nanomanganites. *Nano Stud.—Sci. J.* **2016**, *13*, 7–13.
60. Solt, H.E.; Németh, P.; Mohai, M.; Sajó, I.E.; Klébert, S.; Franguelli, F.P.; Fogaca, L.A.; Pawar, R.P.; Kótai, L. Temperature–Limited Synthesis of Copper Manganites along the Borderline of the Amorphous/Crystalline State and Their Catalytic Activity in CO Oxidation. *ACS Omega* **2021**, *6*, 1523–1533. [[CrossRef](#)] [[PubMed](#)]
61. Pollert, E. Tetragonal–to–cubic transformation of hausmannite. *J. Solid State Chem.* **1980**, *33*, 305–308. [[CrossRef](#)]
62. Miyahara, S. Jahn–Teller distortion in magnetic spinels. *J. Phys. Soc. Japan* **1962**, *17* (Suppl. B1), 181–184.

63. Radhakrishnan, N.K.; Biswas, A.B. A Neutron Diffraction Study of Cation Distribution in Some Manganites. *J. Ind. Chem Soc.* **1974**, *37*, 274–281.
64. Sinha, A.P.B.; Sanjana, N.R.; Biswas, A.P.B. The crystal structure of copper manganite. *J. Phys. Chem.* **1958**, *62*, 191–194. [[CrossRef](#)]
65. Waskowska, A.; Gerward, L.; Olsen, J.S.; Steenstrup, S.; Talik, E. CuMn<sub>2</sub>O<sub>4</sub>: Properties and the high-pressure induced Jahn–Teller phase transition. *J. Phys. Condens. Matter* **2001**, *13*, 2549–2562. [[CrossRef](#)]
66. Dorris, S.E.; Mason, T.O. Electrical Properties and Cation Valencies in Mn<sub>3</sub>O<sub>4</sub>. *J. Am. Ceram. Soc.* **1988**, *71*, 379–385. [[CrossRef](#)]
67. Vetter, K.M.; Manecke, G. Der Einstellungsmechanismus des Mn<sup>+++</sup>/Mn<sup>++++</sup>-Redoxpotentials an Platin. *Z. Phys. Chem.* **1950**, *195*, 270–337. [[CrossRef](#)]
68. Buhl, R. Manganites spinelles purs d'elements de transition preparations et structures cristallographiques. *J. Phys. Chem. Solids* **1969**, *30*, 805–812. [[CrossRef](#)]
69. Blasse, G. Ferromagnetism and ferrimagnetism of oxygen spinels containing tetravalent manganese. *J. Phys. Chem. Solids* **1966**, *27*, 383–389. [[CrossRef](#)]
70. Miller, A. Determination of the valence state of copper in cubic CuMn<sub>2</sub>O<sub>4</sub> spinel by X-ray absorption edge measurements. *J. Phys. Chem. Solids* **1967**, *29*, 633–639. [[CrossRef](#)]
71. Lenglet, M.; D'Huysser, A.; Kasperek, J.; Bonnelle, J.P.; Durr, J. Characterization of the oxidation states of copper and manganese in some manganites by the analysis of the XPS spectrum, X emission, and X absorption thresholds. *Mater. Res. Bull.* **1985**, *20*, 745–757. [[CrossRef](#)]
72. Di Castro, V.; Furlani, C.; Gargano, M.; Rossi, M. XPS characterization of the CuO/MnO<sub>2</sub> catalyst. *Appl. Surf. Sci.* **1987**, *28*, 270–278. [[CrossRef](#)]
73. Radhakrishnan, N.K.; Biwas, A.B. A neutron diffraction study of the spinel oxide CuMn<sub>2</sub>O<sub>4</sub>. *Phys. Status Solidi (A) Appl. Res.* **1977**, *44*, 45–49. [[CrossRef](#)]
74. Gillot, B.; Buguet, S.; Kester, E.J. Oxidation mechanism and valence states of copper and manganese in tetragonal CuMn<sub>2</sub>O<sub>4</sub>. *Mater. Chem.* **1997**, *7*, 2513–2517. [[CrossRef](#)]
75. Buciuman, F.C.; Patcas, F.; Hahn, T. Synergy effect between copper and manganese oxides in hopcalite catalysts. *Stud. Surf. Sci. Catal.* **2001**, *138*, 315–322.
76. Wang, H.; Lu, Y.; Han, Y.X.; Lu, C.; Wan, H.; Xu, Z.; Zheng, S. Enhanced catalytic toluene oxidation by the interaction between copper oxide and manganese oxide in Cu–O–Mn/γ–Al<sub>2</sub>O<sub>3</sub> catalysts. *Appl. Surf. Sci.* **2017**, *420*, 260–266. [[CrossRef](#)]
77. Zhang, D.; Zhang, L.; Shi, L.; Fang, C.; Li, H.; Gao, R.; Huang, L.; Zhang, J. In situ supported MnO<sub>x</sub>–CeO<sub>x</sub> on carbon nanotubes for the low-temperature selective catalytic reduction of NO with NH<sub>3</sub>. *Nanoscale* **2013**, *5*, 1127–1136. [[CrossRef](#)] [[PubMed](#)]
78. Tanaka, Y.; Takeguchi, T.; Kikuchi, R.; Eguchi, K. Influence of preparation method and additive for Cu–Mn spinel oxide catalyst on water gas shift reaction of reformed fuels. *Appl. Catal. A Gen.* **2005**, *279*, 59–66. [[CrossRef](#)]

**Disclaimer/Publisher's Note:** The statements, opinions and data contained in all publications are solely those of the individual author(s) and contributor(s) and not of MDPI and/or the editor(s). MDPI and/or the editor(s) disclaim responsibility for any injury to people or property resulting from any ideas, methods, instructions or products referred to in the content.